A STUDY OF INSTRUMENTAL TECHNIQUE FOR THE MEASUREMENT OF SECONDARY FLOWS IN THE BEND OF A CLOSED CONDUIT

Thesis for the Degree of M. S.

MICHIGAN STATE UNIVERSITY
Cornelius Chung - sheng Shih

1957

A STUDY OF INSTRUMENTAL TECHNIQUE FOR THE MEASUREMENT OF SECONDARY FLOWS IN THE BEND OF A CLOSED CONDUIT

By

Cornelius Chung-sheng Shih

AN ABSTRACT

Submitted to the Michigan State University of Agriculture and Applied Science in partial fulfillment of the requirement for the degree of

MASTER OF SCIENCE

Department of Agricultural Engineering

1957

Approved by E. W. Kidder

The development of rotary sprinkler irrigation systems has created an interest in hydraulic studies of rotary sprinklers. One of the major problems is the need for improvement in the water distribution patterns of the sprinklers. It was recognized that one of the important factors in sprinkler distribution is the secondary flows at the bend or elbow in the rotary sprinkler. Therefore it was the aim of this study to attempt a preliminary analysis of secondary flows in the bend.

For the further purpose of the study, the following preliminary tests were undertaken as the objectives of this dissertation.

1) The method of visualizing secondary flow in the bend of sprinkler.

2) To determine the proper size of manometer tube to indicate static and dynamic heads of water flow in a closed conduit.

3) To determine the proper size of Pitot-static tube for the study of velocity distribution in the bend of a plastic transparent tube.

4) To calibrate the manometer tubes.

5) To develop the correction method of projected area by traversing Pitot-static tube stem into the section.

6) To determine Pitot-static tube coefficients with respect to velocity change.

An effective method to show up the secondary flows in the boundary close to the wall of the plastic tube was found.

The secondary flow patterns were clearly visible on the inside wall of the tube coated with fresh white paint or with black and adhesive oil which was eroded by the flow to show the spiral streamlines. The air-bubble method was successfully used to show the phenomena of streamlines of interior flow. Five mm regular soft glass tube was selected for the construction of vertical piezometer tubes, 30 degree inclined mercury manometers, and 30 degree inclined piezometer tubes.

The suitable size of Pitot-static tube was determined as 0.030 inch I.D. because of its high efficiency in measuring velocity and the negligible effect of water viscosity to the flow in the Pitot-static tube.

The non-uniform variation of capillary rise necessitated the calibration of the manometer. The error of time lag on the readings was eliminated by allowing two minutes to elapse, thus establishing stable reading in the manometer.

The double traversing method made possible the use of a constant correction for the projected area of the traversing Pitot-static tube stem along a diameter of the plastic tube, and it was used to determine the velocity distribution curves in the sections.

The ratios of the mean velocities obtained from the velocity distribution curves, to the mean velocities obtained from weighing method was applied for drawing calibration curves of the Pitot-static tube coefficients with respect to velocity changes.

Each of the author's four Pitot-static tubes had its individual coefficient calibration curve as shown in Fig. 24. The slopes of the four calibration curves were approximately the same.

A STUDY OF INSTRUMENTAL TECHNIQUE FOR THE MEASUREMENT OF SECONDARY FLOWS IN THE BEND OF A CLOSED CONDUIT

By

Cornelius Chung-sheng Shih

A THESIS

Submitted to the Michigan State University of Agriculture and Applied Science in partial fulfillment of the requirement for the degree of

MASTER OF SCIENCE

Department of Agricultural Engineering

1957

6/24/57

ACKNOWLEDGMENTS

The author wishes to express his sincere thanks to Professor Ernest H. Kidder, under whose guidance this project was conducted, for his counsel, encouragement, and helpfulness in making this project a reality. He is greatly indebted to Professor Harold R. Henry of Civil Engineering Department and to Doctor Fred H. Buelow of Agricultural Engineering Department and Doctor Charles O. Harris, Head of the Department of Applied Mechanics, for their assistance.

The author wishes to express his appreciation to Doctor Arthur W. Farrall, Head of the Agricultural Engineering Department, and Doctor Merle L. Esmay of Agricultural Engineering Department for their efforts in arranging for the research assistantship which provided this opportunity for study.

The appreciation is also extended to Messrs. Rolland Z. Wheaton, John J. McDow, Robert A. Aldrich, James L. Butler, Robert W. Kleis, James B. Cawood and Glen Shiffer and all others who provided valuable aid during the conducting of the investigation.

TABLE OF CONTENTS

LIST OF FIGURES

Figure Page

Figure Page

INTRODUCTION

The rapid expansion of irrigation in recent years has been brought about, in part, by the introduction of the portable rotary sprinkler system made up of lightweight aluminum tubing and fittings. The development of rotary sprinkler irrigation systems has created an interest in hydraulic studies of rotary sprinklers. One of the major problems is the need for improvement in the water distribution patterns by rotary sprinklers. There are two desirable distribution patterns which lend themselves well to both overlapping and a simple arrangement of the sprinklers; one is a triangular-shaped pattern, and another is an inverted trapezoidal pattern. However, the sprinklers presently in use do not give completely satisfactory patterns, especially at lower pressures.

Bilanski [10] recognized that one of the important factors in sprinkler distribution is the secondary flow at the bend or elbow in the rotary sprinkler. As the hydraulic pressure and degree of bending are fixed, a decrease in length of extended tube will improve the distribution pattern proportionally while increasing the length will have the opposite result. The intensity of secondary flows will vary with change in the degree of bend and velocity. It was,therefore,the aim of this study to attempt a preliminary analysis

of relationships between secondary flows and the bend under several hydraulic pressures.

For the further purpose of the study, the following preliminary tests were undertaken as the objectives of the dissertation:

(1) to develop a method of visualizing secondary flow in the bend of a sprinkler,

(2) to determine the proper size of manometer tube to use,

(3) to determine the proper size of Pitot-static tube for the study of velocity distribution in the bend of a plastic transparent tube,

(4) to calibrate the manometer tubes,

(5) to develop methods of adjusting error in velocity measurement with Pitot-static tube, which in turn causes a reduction of water flow cross-sectional area as the traversing Pitot-static tube crosses the section,

(6) to determine Pitot-static tube coefficients with respect to velocity change.

FLOW SYSTEM CONSTRUCTION

Flow System No. 1

This system (shown in Fig. 1) was assembled for testing different means of showing secondary flows in the bend of two inches O.D. (1.85" I.D.) plastic transparent tube made of polyethylene, and for measuring time lag for different sizes of manometer tube and Pitot tube. The study was conducted in the Land Development Laboratory in the Agricultural Engineering Building, Michigan State University.

Source of Water: Water was obtained from a concrete storage tank having a capacity of approximately 2500 gallons.

Pump: A vertical turbine-type multistage pump capable of a rate of delivery of 250 gallons per minute at 22 feet of head was used to deliver water from the storage tank to the flow system. The pump was driven by a five horsepower electric motor. The pump discharged at the main floor level A ten foot vertical pump column extended down to the storage tank in the basement.

Pressure Surge Tanks: The pump was connected by a 1 3/4" diameter iron pipe to two 55 gallon surge tanks. The tanks were connected by a 3/4" diameter pipe as shown in Fig. 1 and Fig. 2.

Two globe valves were placed in the discharge line to control the pressure.

Delivery of Water to the Bend: A one inch I.D. rubber hose six feet long made a flexible connection from the surge tanks

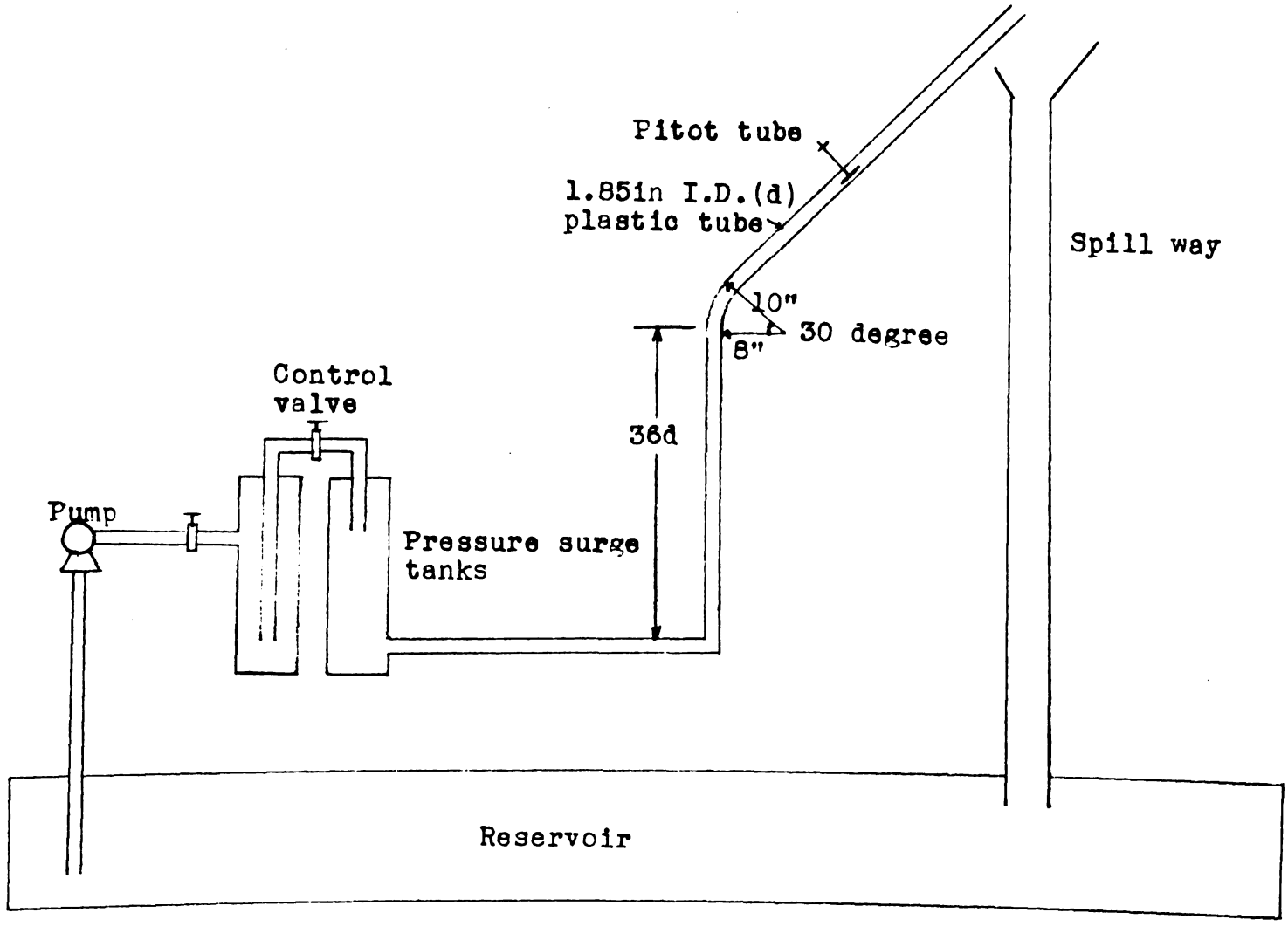

Fig. 1. Schematic diagram of flow system No. 1

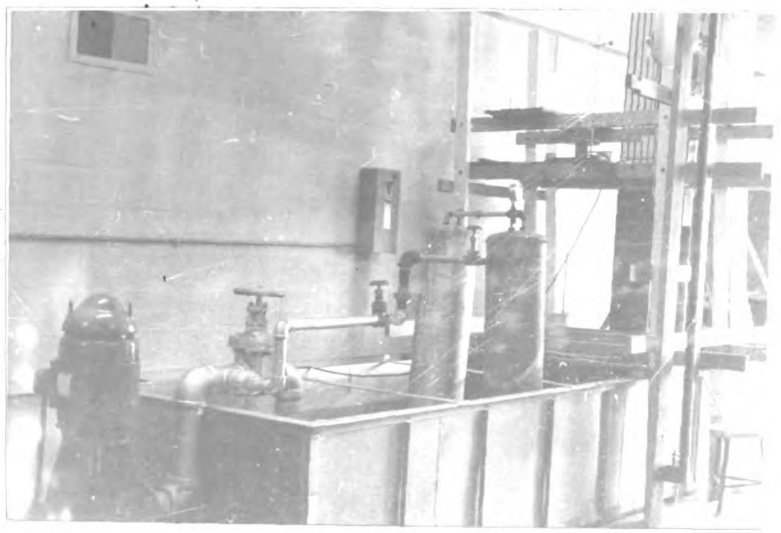

Fig. 2. View of flow system No. 1

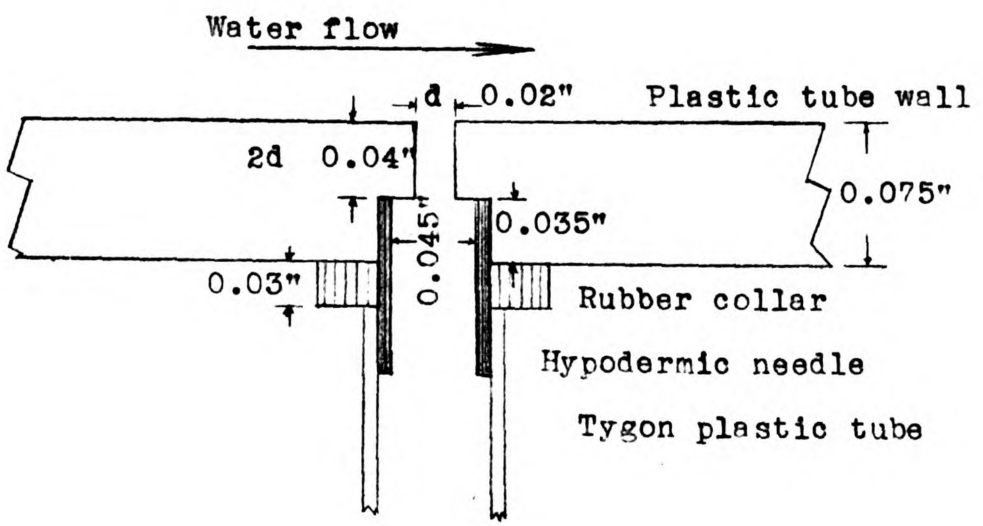

Fig. 3. Piezometer opening Profile

to a vertical stand pipe of 1 3/4" diameter (nominal) by five feet long. The two inch O.D. bent plastic tube was connected by a rubber hose of two inches I.D. to the vertical stand pipe. The connection of the mercury manometer (model AF200, maximum pressure 200 psi, King Eng. Corp.) was located one foot from the upper end of the iron vertical stand pipe.

Bent Plastic Transparent Tube: A two inch diameter straight plastic tube five feet long was bent to a 30° turn with ten inches and eight inches outside and inside radius of curvature respectively. The method of bending was by heating with a sand filling in order to keep a uniform cross-section. The bent section was located 1.5 feet from the upstream end and 3.5 feet from the downstream end of the tube.

In order to investigate the static-pressure distribution around the inlet section of the tube, four static pressure probes were stuck into the wall of the tube at a section six inches upstream from the bend. Four mm (0.12 inch I.D.) piezometer tubes were connected to the probes. The structure of a probe is shown in Fig. 3.

Spillway: The water outflow from the vertically mounted bent tube discharged onto a spillway to be returned to the storage tank.

Flow System No. 2

This system was used to determine the velocity coeffi-

cient for Pitot tubes and visualization of secondary flow in the bend.

This system was assembled in the Land Development Laboratory in the basement of the Agricultural Engineering Building.

Source of Water: Water was obtained from a concrete storage tank having a capacity of about 2500 gallons.

Pump: A horizontal centrifugal pump capable of a rate of delivery of 150 gallons per minute at 160 feet head was used to deliver the water from the storage tank to the system. The pump was driven by a ten horsepower electric motor. The pump and motor unit were situated on top of the storage tank as shown in Fig. 4.

Constant Head Tanks: Two 55 gallon open-top tanks connected to each other by two conduits were supplied with water from the storage tank by the pump as shown in Fig. 5. One of the tanks received water from the pump. A screen was provided at the end of the pipe extending from pump into the tank to reduce turbulent water circulation in the tank by the jetting effect. The second tank obtained its water from the receiving tank. It had a sharp-edged weir near the top to keep a proper constant head. The width of this weir was 4/10 of the tank circumference. A gravel section was set in the second tank to retard the water surge from the first tank through the conduits. A hook gage was mounted on this second tank which supplied water to the two inch diameter plastic tube

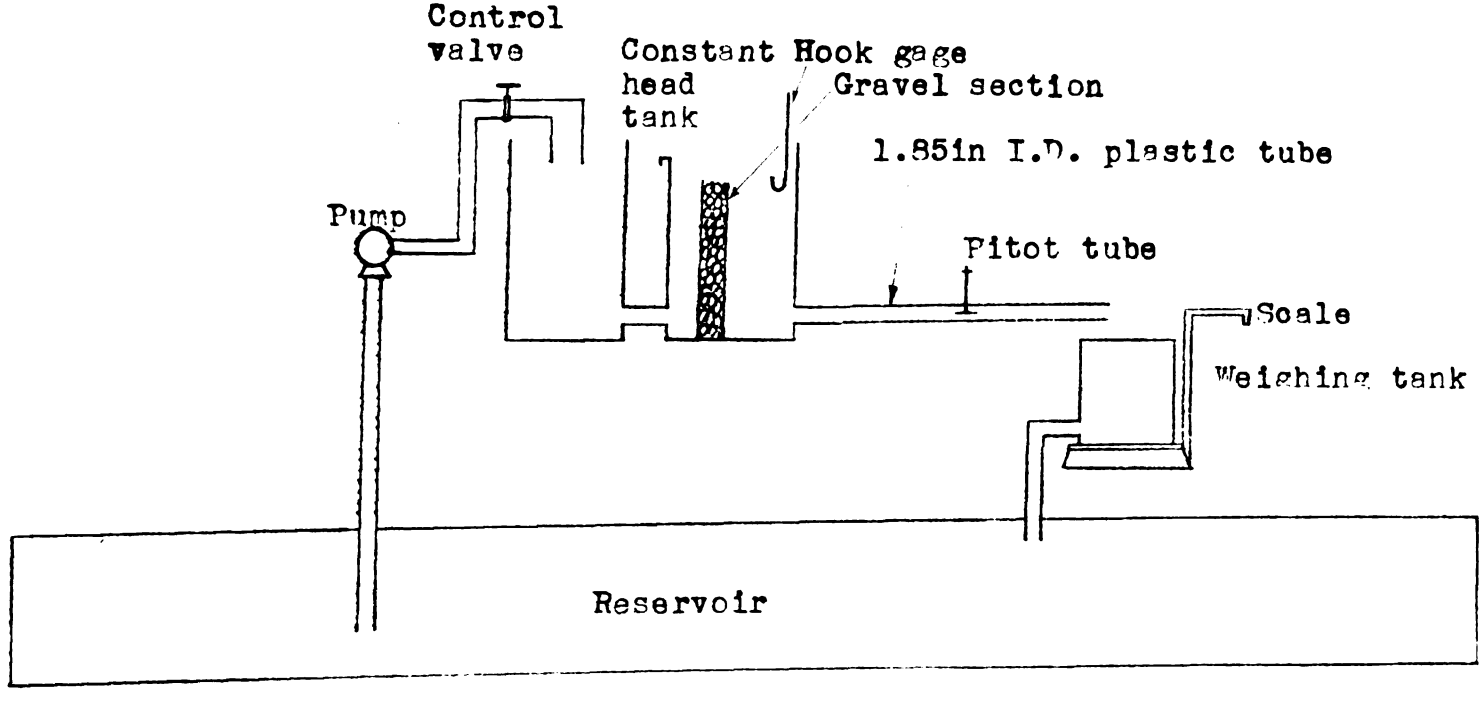

Fig. 4. Schematic diagram of flow system No. 2

used for the Pitot tube measurement, in order to measure the elevation of water surface. A thermometer was placed in the discharge tank. Three round orifices were provided in the wall of the second tank at different levels. This made possible three locations for the plastic tube for operation under 3 static heads.

Plastic Tubes: A two inch diameter plastic transparent tube four feet long was prepared to receive the water supply from the constant head tank for measuring velocity distribution at several sections in the tube. A bell-shaped nozzle was attached at the inlet of the tube to provide a smooth entry flow (Fig. 6). The sections for measuring velocity distribution were at 10 and 15 and 19 diameters of the tube from the inlet. A rubber hose was attached to the outlet of the tube in order to divert water flow in or out of a 40 gallon weighing tank. The static pressures on the tube wall were measured at the points one diameter upstream and downstream from the gaging section in the plastic tube by static pressure probes with piezometer tubes. The structure of the probe are shown in Fig. 3 which were used in flow systems No. 1 and No. 2.

Fig. 5. View of flow system No. 2.

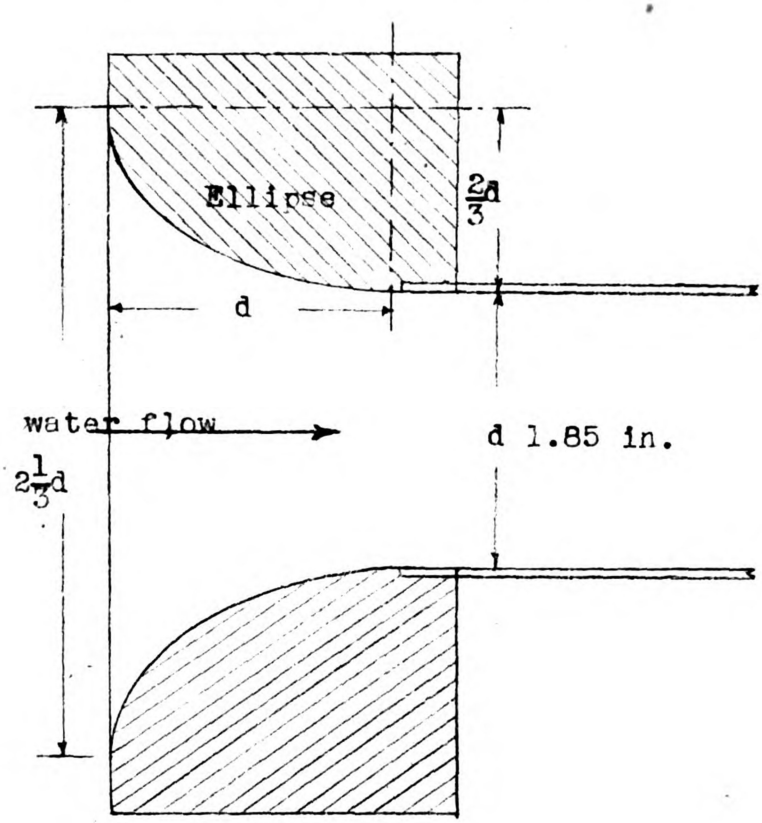

Fig. 6. Bell-shaped nozzle profile

THE CONSTRUCTION OF MANOMETERS

For the velocity and static pressure measurement in this study a double-column manometer, or U tube, and piezometer tubes, or single-column manometer, were constructed. There were two important problems in the selection of a proper size of manometer suitable for this study because of the wide range of flow velocity from about one to ten feet per second; one problem was the time lag which affects the time efficiency of test, and the other was the problem of variable capillary effect in a tube of non uniform diameter.

In order to eliminate the errors that occurred from these two effects, four different sizes of glass tube were selected for study to determine the proper bore size of manometer tube. Also two different sizes of Pitot tube were attached to some of these monometers to study the dynamic responses related to the time lags.

Detailed calibration of the selected manometer was necessary on account of the variable capillary effect in the tube of slightly variable diameter.

When water flows under turbulent conditions, the manometer will rarely give a perfectly steady reading. Its surface will oscillate irregularly through a range of several millimeters, with a periodicity of perhaps 1/4 or 1/2 second, and there may be occasional surges of greater amplitude. To make a completely accurate estimate of the mean position of the column was

beyond the power of the observer, and therefore two damping methods; capacity damping by mercury and resistance damping by screw clamps; were applied to bring the indicating column nearly to rest. The use of 30 degree inclined manometer board increased the reading accuracy twice that of a vertical board.

Above all, the error due to time lag was practically eliminated by estimating two minutes time lag for five mm manometer tubes.

A THEORETICAL ANALYSIS OF TIME LAG

The piezometer tube or manometer is generally considered as a second-order-type instrument for the dynamic responses. The second order term is due to the inertia of the mass in the manometer tube. But if the diameter size of manometer tube is small and the mass becomes small enough, then the instrument will behave more like a first-order type. The first order term results from the viscous resistance to flow. As the manometer possesses a dynamic response to a step change that may ideally be described by means of a second-order differential equation which is derived from the continuity equation and the momentum equation. The continuity equation between Pitot tube and manometer is expressed as follows:

$$V_p = V_m \frac{A_m}{A_p} \qquad (1)$$

Where V_p = velocity in Pitot tube

V_m = velocity in the manometer tube

A_p = cross-sectional area of Pitot tube

A_m = cross-sectional area of manometer tube.

Then momentum equation for the flow in manometer with connecting tube and Pitot tube is derived as:

$$\rho A_p \frac{dV_p}{dt} L = \gamma (h_f - h) A_p - \tau_0 (W.P.) L$$

$$\rho L \frac{dV_p}{dt} = \gamma (h_f - h) - \gamma h_L$$

$$\frac{L}{g} \frac{dV_p}{dt} = h_f - h - h_L \qquad (2)$$

where L = length of Pitot tube plus corrected lengths of connecting tube and water in manometer,

ρ = density of water,

γ = specific weight of water,

h_f = final steady pressure head indicated by manometer,

h = pressure head indicated by manometer,

h_L = pressure head loss in the system,

τ_0 = intensity of shear between water flow and the tube wall,

W.P. = wetted perimeter of Pitot tube

g = gravitational acceleration,

t = time

If it is assumed that there is a laminar flow in the Pitot tube and manometer, then

$$h_L = C_1 V_p + C_2 V_m + C_3 V_c \qquad (3)$$

and $$h_L \cong C_1 \frac{A_m}{A_p} V_m \qquad (4)$$

When the friction coefficient of Pitot tube, C_1 is larger than that of manometer C_2 and of connecting tube C_3.

$C_1 \frac{A_m}{A_p}$ may be expressed as C

Hence $$V_m = \frac{dh}{dt} \quad \text{and} \quad \frac{dV_m}{dt} = \frac{d^2h}{dt^2}$$

The momentum equation is expressed as follows:

$$\frac{L}{g} \frac{A_m}{A_p} \frac{d^2h}{dt^2} = h_f - h - C \frac{dh}{dt} \qquad (5)$$

if assume $\frac{L}{g} \frac{A_m}{A_p} \cong a_2$, C is a_1, as a constant.

$$a_2 \frac{d^2h}{dt^2} + a_1 \frac{dh}{dt} + h = h_f \qquad (6)$$

The solution to this second-order differential equation (6) involves three cases: an oscillatory condition in which the roots of the auxiliary equation are conjugate complex with negative real parts: critical damping in which the roots are negative, real and equal: and an overdamped condition in which the roots are negative, real and unequal.

The particular solutions for given initial conditions are:

1. Oscillatory response $\zeta < 1$;

$$\frac{h}{h_f} = 1 - \frac{1}{\sqrt{1-\zeta^2}} e^{-\frac{t}{T_2}\zeta} \cos\left[\frac{\sqrt{1-\zeta^2}}{\zeta}\frac{t}{T_2} - \phi\right] \qquad (7)$$

where $T_2 = \frac{2a_2}{a_1}$ = characteristic time

$\zeta = \sqrt{\frac{a_1^2}{4a_2}}$ = damping ratio

ϕ = arc sin (ζ)

2. Critically damped response, $\zeta = 1$:

$$\frac{h}{h_f} = 1 - e^{-\frac{t}{T_2}}\left[1 + \frac{t}{T_2}\right] \qquad (8)$$

3. Overdamped response, $\nu > 1$:

$$\frac{h}{h_f} = 1 - \frac{\nu}{\nu-1} e^{\frac{-2}{\nu+1}\left(\frac{t}{T_2}\right)} + \frac{1}{\nu-1} e^{\frac{-2\nu}{\nu+1}\left(\frac{t}{T_2}\right)} \qquad (9)$$

where $$\nu = \frac{1+\sqrt{1-\left(\frac{4a_2}{a_1^2}\right)}}{1-\sqrt{1-\left(\frac{4a_2}{a_1^2}\right)}} = \text{damping number}$$

The time lag is directly proportional to the characteristic time T2: a larger characteristic time, T2 produces a greater time lag and a slower response. In addition, an increase in damping ratio ζ or an increase in damping number ν also increases the time lag and makes the response

slower. Therefore two numbers such as T_2 and ζ or ν are required to express the time lag of a manometer. When the mass acceleration existing in the manometer, due to the step change of pressure head, is extremely small, the manometer will behave more like a first-order type. Ideally the dynamic response of first-order type instruments to a step change of pressure head can be represented by,

$$a_1 \frac{dh}{dt} + h = h_f \qquad (10)$$

In comparison to the second-order differential equation (6), Constant a_2 is assumed to be zero, or practically approach zero, because the second derivative term in the equation (6) represent the acceleration mass. If the constant a_1 is called a time constant T_1, this linear first-order differential equation has the particular solution for given initial condition,

$$\frac{h}{h_f} = 1 - e^{-\frac{t}{T_1}} \qquad (11)$$

As the time constant T_1, which is a measure of time lag, becomes larger, the response, while maintaining the same shape, becomes proportionately slower. The time constant T_1 is the time required to indicate 63.2 per cent of the complete change and is numerically equal to the product of resistance, C_1, and capacitance, $\frac{Am}{AP}$.

In this case, the second-order type instrument behaves like a first order type, as the constant a_2 becomes a zero or approaches zero in an overdamped condition. It is proved by

the following mathematical treatment, in equation (9)

$$\frac{h}{h_f} = 1 - \frac{\nu}{\nu-1} e^{\frac{-2}{\nu+1}\left(\frac{t}{T_2}\right)} + \frac{1}{\nu-1} e^{-\frac{2\nu}{\nu+1}\left(\frac{t}{T_2}\right)}$$

as $a_2 \to 0$ $\qquad \nu = f(a_2)$

$$\lim_{a_2 \to 0} \nu = \infty$$

then $\frac{1}{\nu-1} = 0$ $\qquad \frac{\nu}{\nu-1} = 1\frac{\infty}{\infty}$: indeterminate

$$\frac{t}{T_2} \cdot \frac{(-2)}{\nu+1} = \frac{-tT_1}{2}\left(\frac{1-\sqrt{1-\frac{4a_2}{a_1^2}}}{a_2}\right)$$

$$= \frac{-tT_1}{2}\left(\frac{0}{0}\right) \quad : \text{indeterminate.}$$

The indeterminate form is solved as follows according to L' Hospital's rule.

$$\text{if} \quad f(a_2) = 1 - \sqrt{1-\frac{4a_2}{a_1^2}}$$

$$g(a_2) = a_2$$

$$\lim_{a_2 \to 0} \frac{f(a_2)}{g(a_2)} = \frac{f'(a_2)}{g'(a_2)} = \frac{\left(1-\frac{4a_2}{a_1^2}\right)^{-\frac{1}{2}}\left(\frac{2}{a_1^2}\right)}{1}$$

$$= \frac{2}{a_1^2} = \frac{2}{T_1^2}$$

Therefore

$$-\frac{t}{T_2} \cdot \frac{2}{\nu+1} = -\frac{tT_1}{2} \cdot \frac{2}{T_1^2} = -\frac{t}{T_1}$$

Thus the equation (9) reduces to the first-order equation (11) when α_2 becomes zero or approaches zero.

The friction factor C is obtained by the following equation,

$$C = C_1 \frac{A_m}{A_p}$$

It is assumed that laminar flow exists in the Pitot tube and manometer. $h_L \cong C_1 V_p \cong \left(\frac{64}{Re}\frac{L}{d_p} + Ke\right)\frac{V^2}{2g} = \left(\frac{32 L \mu}{Re\, d_p^2 g} + Ke\frac{V_p}{2g}\right)V_p$

$$C_1 = \left(\frac{32\mu L}{\gamma d_p^2} + Ke\frac{V_p}{2g}\right) \qquad (12)$$

$$\text{hence } C = \left(\frac{32\mu L}{\gamma d_p^2}\frac{A_m}{A_p} + Ke\frac{V_p}{2g}\frac{A_m}{A_p}\right) \qquad (13)$$

Where μ = viscosity of water

d_p = inside diameter of Pitot tube

R_e = Raynold's number in the Pitot tube

K_e = form resistance coefficient at the entry of Pitot tube.

B. Experimental Analysis of Time Lag.

The test for the measurement of time lag was conducted with flow system No. 1. The experimental results were shown in Fig. 7a, 8, and 9.

In Fig. 7a, three mm capillary tube, five mm glass tube and seven mm glass tube, on 30 degree inclined manometer board, resulted in different time lags due to the variation of tube size and Pitot tube size, where 0.030 inch I.D. and 0.0215 inch I.D. Pitot tubes were applied at a given velocity of 1.5 fps.

In Fig. 8, the time lag of five mm and seven mm glass tubes on the vertical manometer board were tested respectively at a given velocity of two fps and 3.6 fps with 0.030 inch I.D. Pitot tube and 0.0215 inch I.D. Pitot tube.

In Fig. 9, the time lag for mercury manometer, (5 mm double column manometer) was tested on a 30 degree inclined board at a velocity of 6.89 fps. The time lag due to the pressure change caused by shifting the position of Pitot orifice along the traversing line in the tube section, was investigated and shown in Fig. 9. This time lag behavior was similar to the initial time lag. It was noted that apparently most of the time lag curves represented overdamped response.

In Fig. 7b, the experimental time lag curves of five mm (0.12 inch I.D.) and seven mm (0.21 inch I.D.) glass tubes with 0.030 inch I.D. and 0.0215 inch I.D. Pitot tubes were

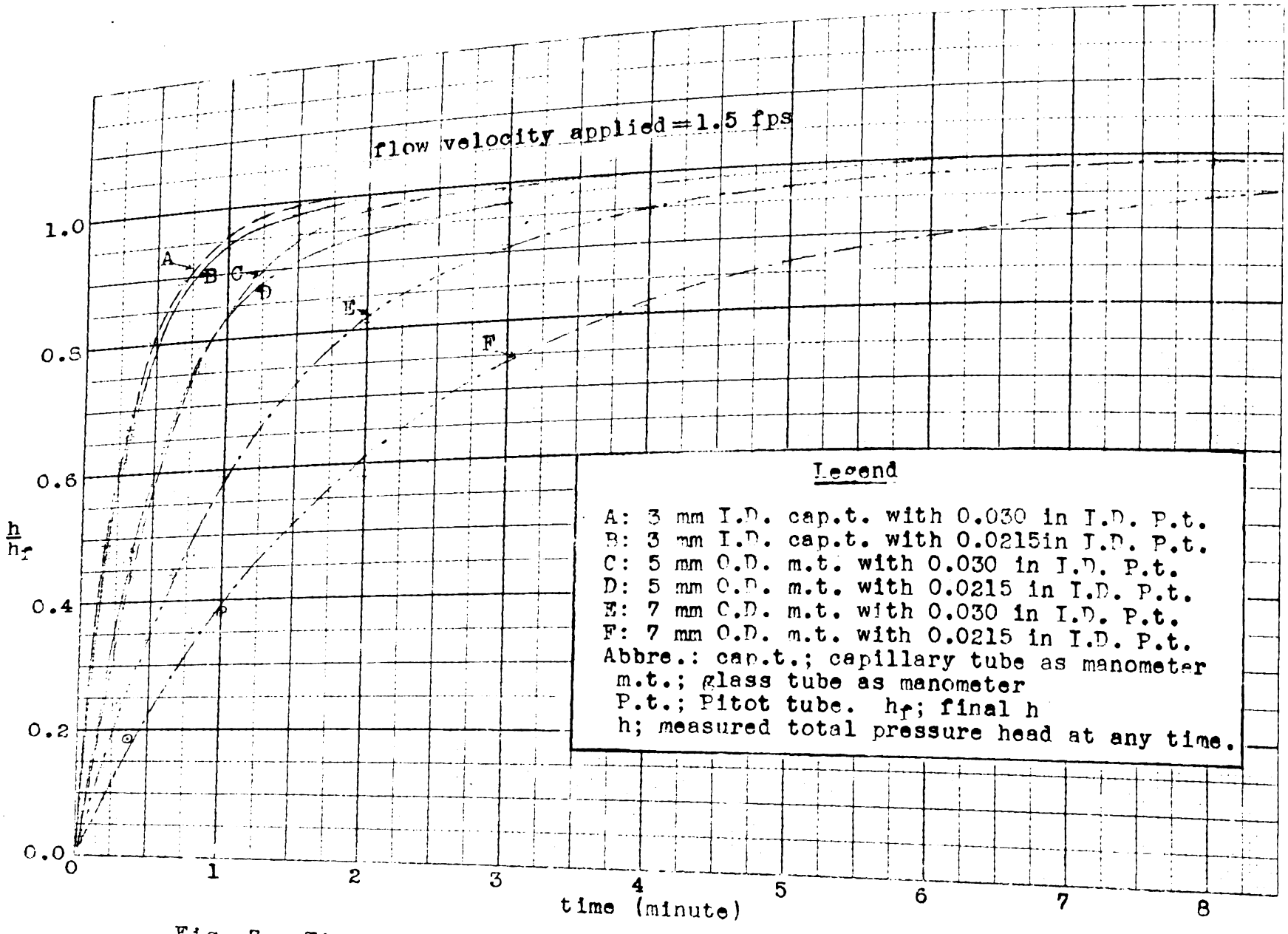

Fig. 7a. Time lag curves for three sizes of manometer tubes on 30 degree inclined board with two sizes of Pitot tubes.

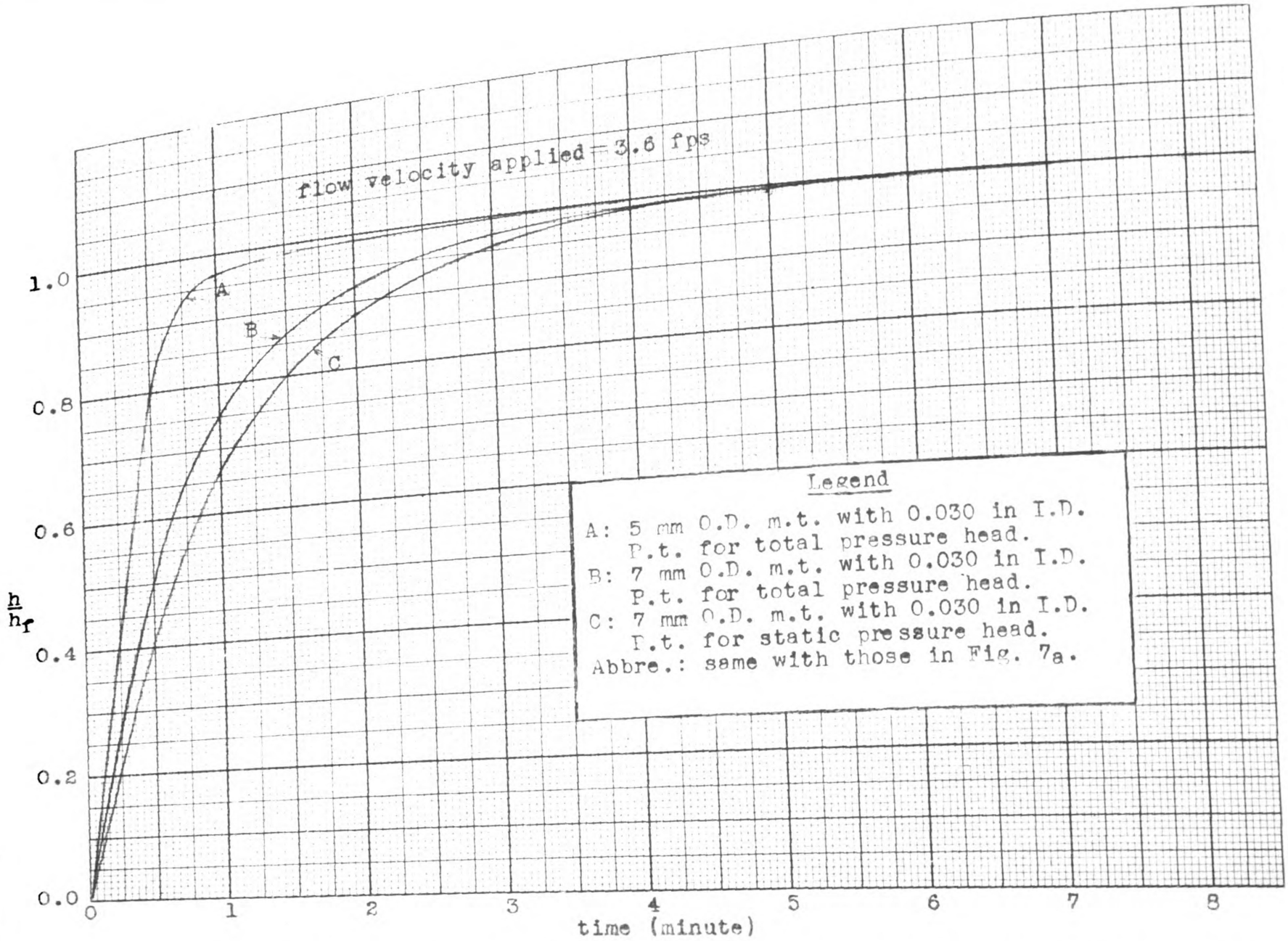

Fig. 8. Time lag curves for two manometer tube sizes on vertical board with one Pitot tube size.

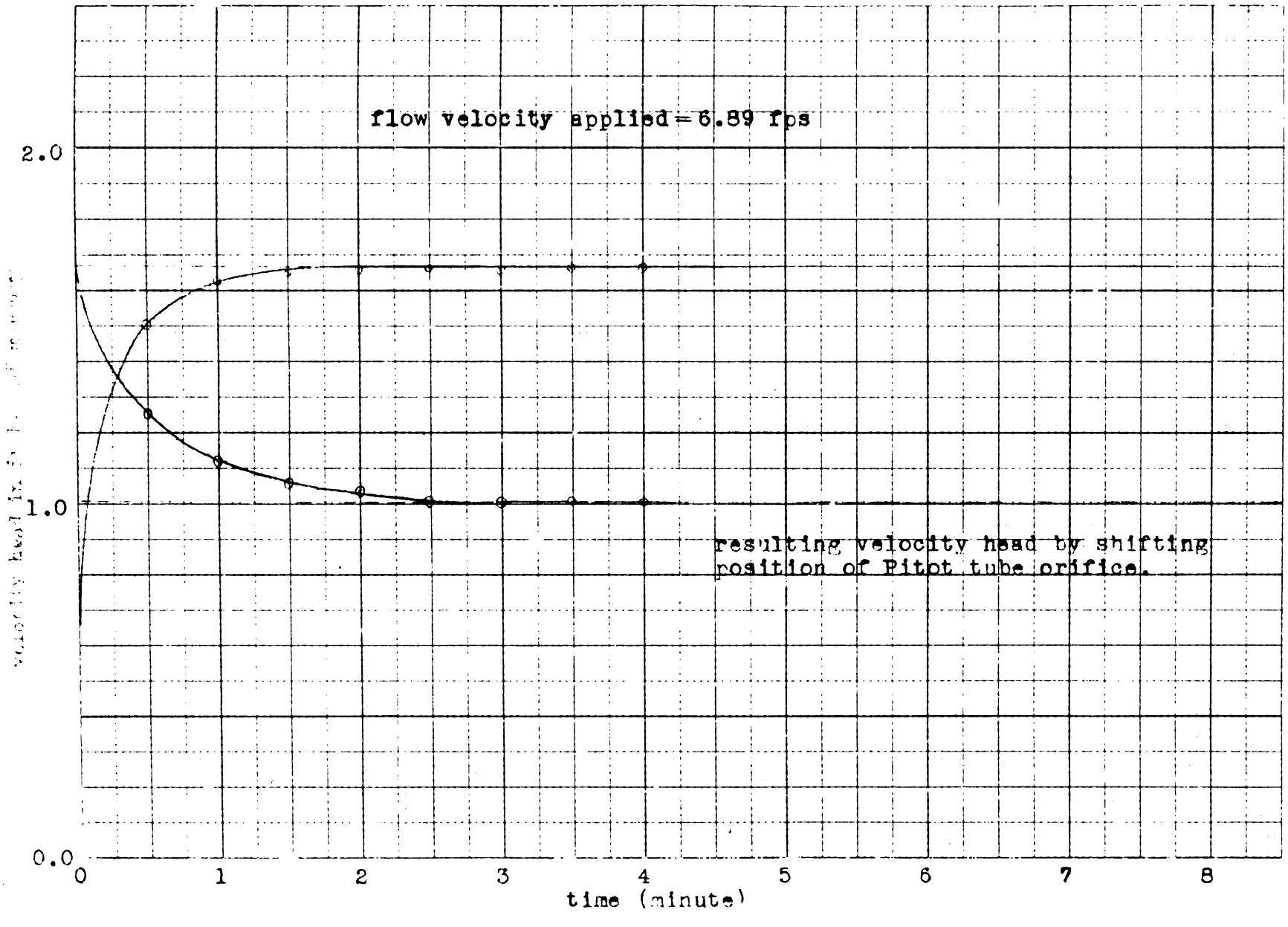

Fig. 9. Time lag curves for mercury manometer(double column) on 30 degree inclined board.

drawn with the theoretical curves for comparison.

According to equation (9) for the case of overdamped response in second-order-type manometer,

$$\frac{h}{h_f} = 1 - \frac{\nu}{\nu-1} e^{\frac{-2}{\nu+1}\cdot\frac{t}{T_2}} + \frac{1}{\nu-1} e^{\frac{2\nu}{\nu+1}\cdot\frac{t}{T_2}}$$

where $\nu = \dfrac{1+\sqrt{1-(4a_2/a_1^2)}}{1-\sqrt{1-(4a_2/a_1^2)}}$ = damping number

Since

$$a_1 = C = T_1 = \text{time constant}$$

$$a_2 = \frac{L d_m^2}{g d_p^2}$$

$$C_1 = C\frac{A_p}{A_m} \quad ; \quad C = C_1\frac{A_m}{A_p}$$

$$T_2 = \frac{2a_2}{a_1} = \frac{2L d_m^2}{C g d_p^2}$$

$$C = \left(\frac{32\mu L}{\gamma d_p^2} + K_e\frac{V_p}{2g}\right)\frac{A_m}{A_p} = \left(\frac{32\mu L}{\gamma d_p^2} + K_e\frac{V_p}{2g}\right)\frac{d_m^2}{d_p^2}$$

If K_e is assumed to be 0.5, referring to "Fluid Mechanics" by J. K. Vennard, p. 217 - 218 (square-edged entrence).

Also assume $V_p \leqq 1.5$ feet per second

then $K_e\frac{V_p}{2g} \leqq 0.01165$

If K_e is assumed to be 0.8 for the case of reentrant entrance, (from the same reference as the above)

also $V_p \leqq 1.5$ feet per second,

then $K_e\frac{V_p}{2g} \leqq 0.0186$

Hence the term, $K_e\frac{V_p}{2g}$, is small enough to be neglected, thus,

then
$$C = \frac{32\mu L d_m^2}{\gamma d_p^2 \cdot d_p^2} = T_1 \qquad (14)$$

$$L = \frac{C\gamma d_p^4}{d_m^2 32\mu} \qquad (15)$$

As time constants, T_1, are obtained from experiment as shown in Fig. 7a. L can be determined.

Also, according to equation (11) for first-order-type manometer,

$$\frac{h}{h_f} = 1 - e^{-\frac{t}{T_1}}$$

T_1 may be obtained from experimental data. The equation (9) and (11) with the time constant, T_1, or coefficient C obtained from experimental data, were employed for drawing the theoretical time lag curves for second and first-order type manometer, in order to make a comparison with experimental curves.

If the following values are substituted in equation (15):

d_m = 0.12 inch (I.D., manometer tube)

d_p = 0.030 inch (I.D., Pitot tube)

$T_1 = C = 18$ sec (obtained from experimental curve in Fig. 7a.)

then $$L = \frac{18 \times 62.4 \times \left(\frac{0.03}{12}\right)^4}{32 \times 2.7 \times 10^{-5} \times \left(\frac{0.12}{12}\right)^2} = 0.508 \text{ feet}$$

since viscosity $U = 2.7 \times 10^{-5} = \text{lb sec/ft}^2$ (at 52°F)

$$T_2 = \frac{2 \times 0.508 \times (0.12)^2}{18 \times 32.2 \times (0.03)^2} = 0.0276 \text{ sec}$$

$$= \frac{1 + \sqrt{1 - (0.00307)}}{1 - \sqrt{1 - (0.00307)}} = 1249$$

For second-order-type manometer:

$$\frac{h}{h_f} = 1 - \frac{1249}{1248} e^{-\frac{2t}{1250 \times 0.0276}} + \frac{1}{1248} e^{-\frac{2498t}{1250 \times 0.0276}}$$

$$\cong 1 - e^{-0.058t} \qquad (16)$$

For first-order type manometer:

$$\frac{h}{h_f} = 1 - e^{-\frac{t}{T}} = 1 - e^{-0.0556t} \qquad (17)$$

The equations (16) and (17) showed the similarity of the two types of curves.

In Fig. 7b theoretical time lag curves for equation (16) and (17) were drawn to compare with the experimental curve for each type manometer. The experimental time lag curves of 0.12 inch I.D. manometer with 0.030 inch I.D. Pitot tube and with 0.0215 inch I.D. Pitot tube respectively, 0.21 inch I.D. manometer with 0.030 inch I.D. Pitot tube and with 0.0215 inch I.D. Pitot tube respectively were applied in Fig. 7b, for the comparison with the theoretical curves.

In Fig. 7b most of the experimental curves tend to behave as the first-order-type curve, however it is theoretically considered as the second-order-type with overdamped response. In equation (14), time constant, T_1, or coefficient, C, is proportionally related to $\frac{dm^2}{dp^2}$ with a constant, K. When $K = \frac{32\mu L}{\gamma}$ (unit in sec-ft^2) where μ, γ, and L are assumed to be constant. From experimental data, the relative curve between T_1 and $\frac{dm^2}{dp^2}$ was plotted in Fig. 10, to obtain the value of L which is the only unknown in the constant K.

From Fig. 10, the value of constant, K, was obtained with the mean relative curve, as 6.9×10^{-6} sec-ft^2. Thus the mean value of L was determined from the equation, $K = \frac{32\mu L}{\gamma}$, as 0.5 ft. for the experiment in this study.

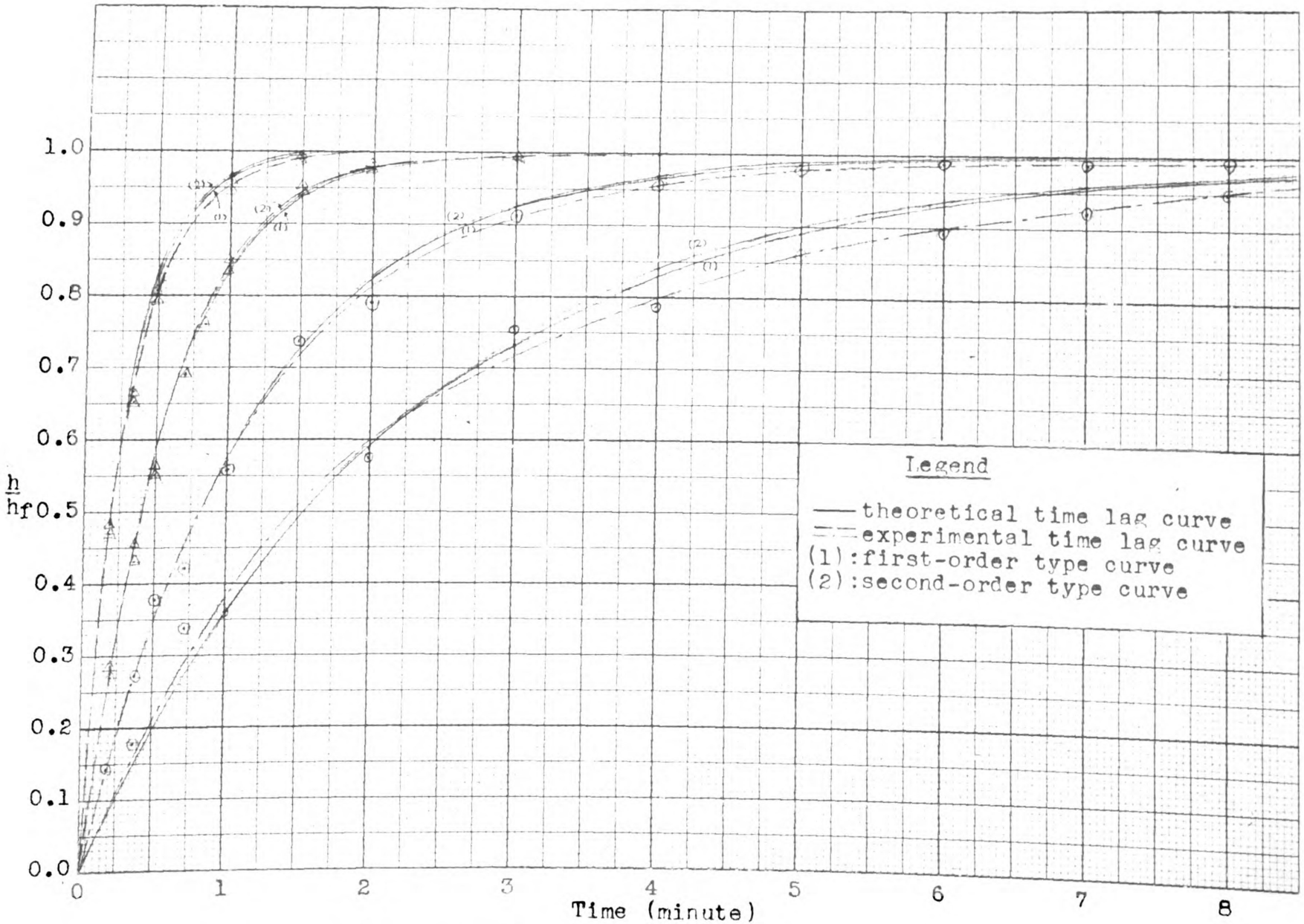

Fig. 7_b. Comparison of theoretical and experimental time lag curves.

The slope of the mean relative curve in Fig. 10 was retained in unity according to theoretical relationship in equation (14). Therefore the least square method was not applied in drawing the relative curve.

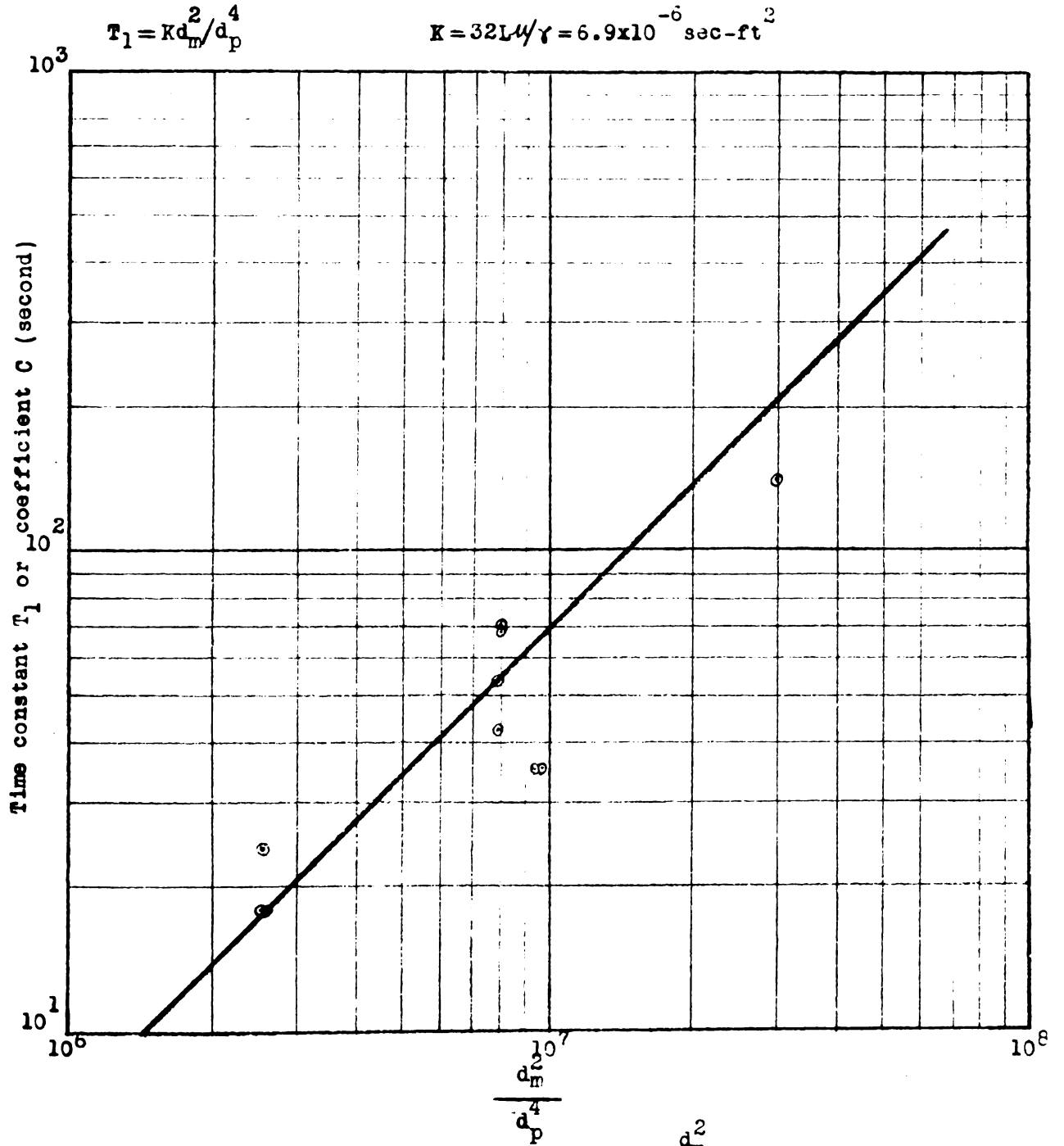

Fig. 10. Relative curve of time constant T_1 to $\frac{d_m^2}{d_p^4}$.

C. Theoretical Analysis of Capillary Effect

Due to the surface-tension of a liquid, liquid in a small tube will form a meniscus" or curved surface in the tube, and the liquid in the tube stands above or below the standard level, depending upon the magnitude of the angle of contact. The "capillary rise" in such a tube may be calculated approximately by considering the equilibrium of the vertical forces on the mass of fluid ABCD (Fig. 12). The fluid above the low point of the meniscus being neglected, the weight of ABCD is given by the following equation:

$$W = \gamma h \frac{\pi d^2}{4} \qquad (18)$$

which act downward. The vertical component, F_σ, of the force due to surface tension is given by

$$F_\sigma = \pi \sigma d \cos\beta$$ if σ is surface tension

which acts upward and is in equilibrium with the downward force. Equating these gives

$$h = \frac{4 \sigma \cos\beta}{\gamma d} \qquad (19)$$ if β is the angle of contact between fluid and wall

allowing the capillary rise to be calculated and confirming the familiar fact that capillary rise becomes greater as tube diameter is decreased.

If diameter d has a decrease of Δd

then $d' = d - \Delta d$

$$h' = \frac{4 \sigma \cos\beta}{\gamma d'}$$

$$\therefore \frac{4 \sigma \cos\beta}{\gamma} = C = \text{Constant}$$

$$h' = C\frac{1}{d'} \quad . \quad \Delta h = h' - h = C\left(\frac{1}{d'} - \frac{1}{d}\right)$$

$$= C\frac{\Delta d}{d(d-\Delta d)}$$

$$\therefore \Delta d = \frac{\Delta h\, d^2}{C + \Delta h d} \qquad (20)$$

Δd express the variation of diameter with respect to the change of capillary rise.

In the experiment, Δh, change of capillary rise may be measured. Therefore Δd might be obtained by the above equation.

Theoretically, it is expected that the vertical capillary rise in 30 degree inclined manometer tube or any other inclined manometer tube, must reach the same elevation as the capillary rise in the vertical manometer tube. The schematic diagram is shown in Fig. 11.

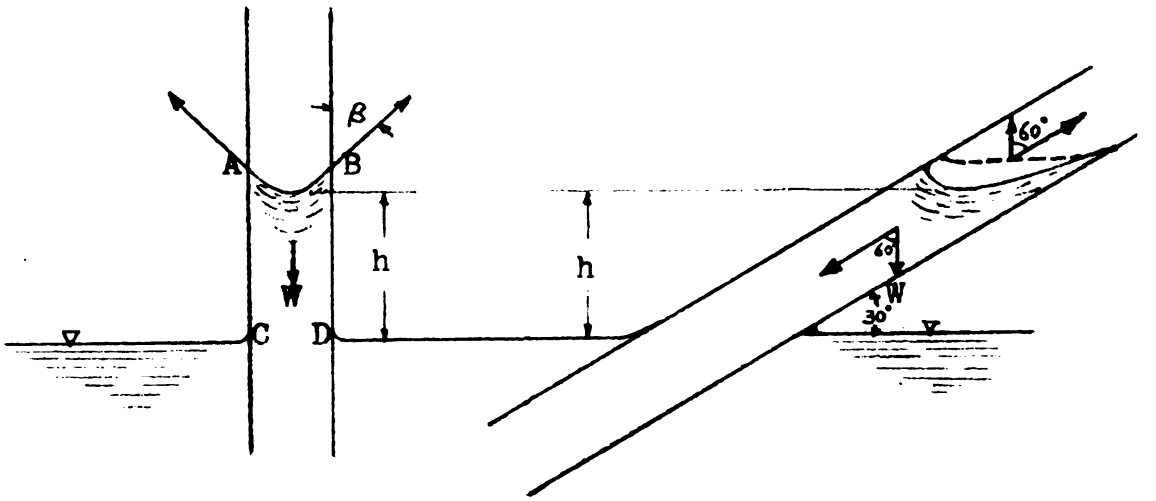

Fig. 11. The capillary effect in the tubes.

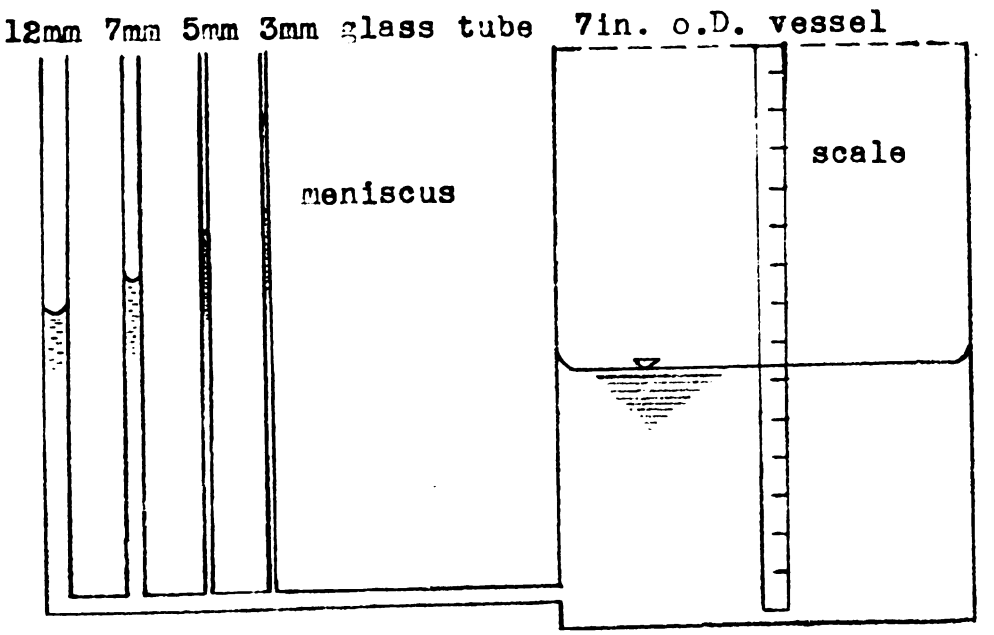

Fig. 12. Schematic diagram of calibration device indicating capillary rise.

D. The Determination of the Size of Manometer.

In pressure head or velocity head measurement by manometer, two important effects must be considered: the first is time lag and the second is capillary rise. Four different sizes of glass tube were tested in this study to make comparison, thus to determine a most suitable size of manometer for the further experiments in velocity and pressure measurement. The four sizes of glass tube were as follows:

1. 3mm capillary tube: 0.119 inch I.D. -0.35 inch O.D.
2. 5mm regular soft glass tube: 0.12 inch I.D. - 0.32 inch O.D.
3. 7mm regular soft glass tube: 0.21 inch I.D. -0.32 inch O.D.
4. 12mm regular soft glass tube: 0.41 inch I.D. -0.53 inch O.D.

Two sizes of Pitot tube made of nickel hypodermic needle were used in this test for determining manometer size (Fig. 13). These Pitot tubes are:

1. 0.0215 inch I.D. Pitot tube
2. 0.030 inch I.D. Pitot tube

The tests were undertaken in flow system No. 1. A capillary rise calibration device was used.

This capillary rise calibration device consisted of a seven inch O.D. vessel, Y-type branches, elevation scale and

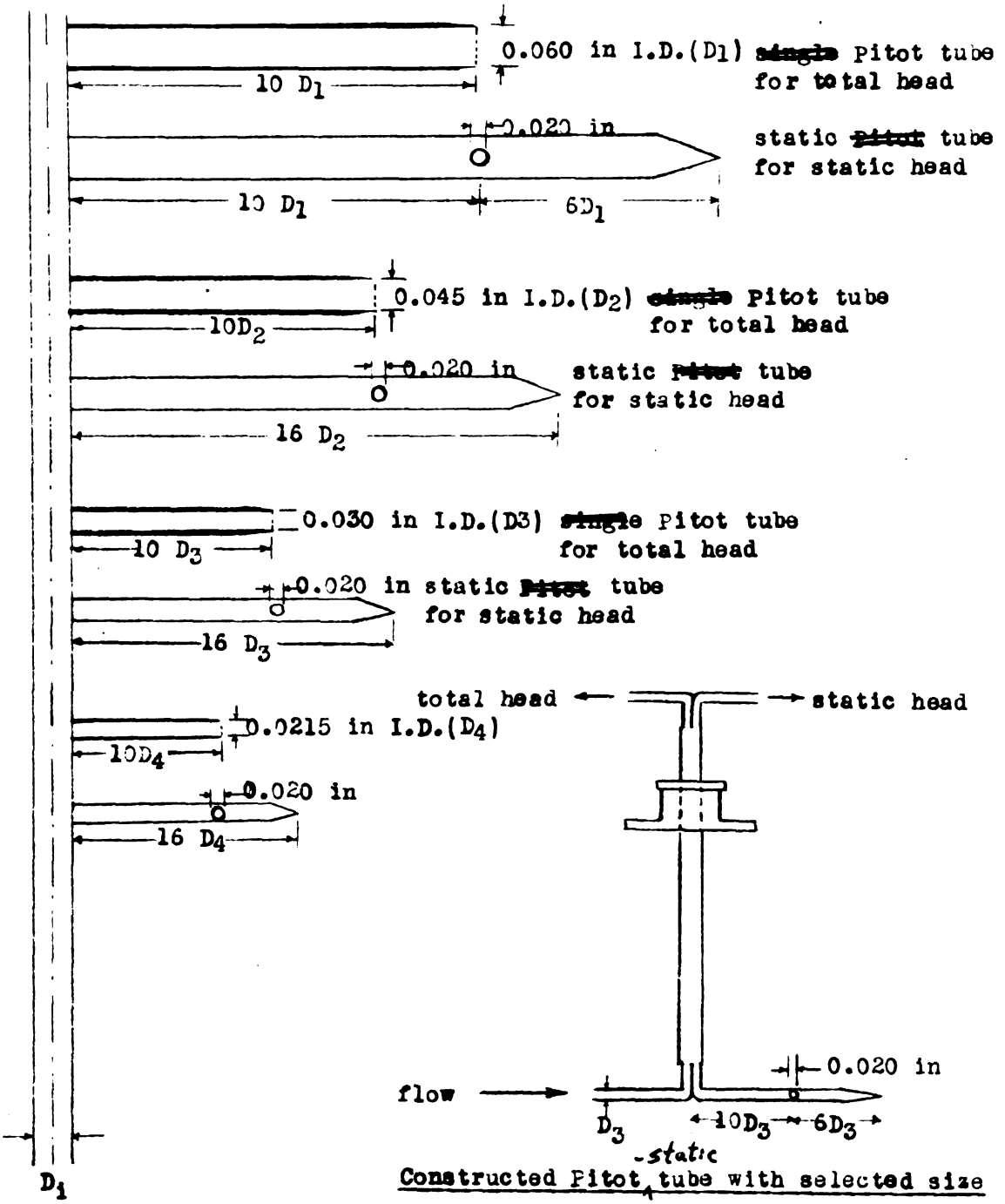

Constructed Pitot tube with selected size

Fig. 13. Diagram of Pitot tube models

rubber connection tubes.(Fig. 12). The measurement of time lag for each glass tube was shown in Fig. 7a, 8, and 9. From those curves of time lags in Fig. 7a it was found that the three mm capillary tube and the five mm glass tube had quite similar time lags, but in the region of 0.9 - 1.0 of $\frac{h_i}{h_f}$, five mm glass tube had a steep slope of the time lag-pressure head curve. Here, h_1 is the total pressure head at each measuring time, h_f is the final total pressure head as it had overcome the time lag. Thus five mm glass tube was determined to be an ideal tube for the manometer from the standpoint of time lag. Time constants, T, of five mm glass tube and three mm capillary tube were approximately the same, about 0.3 minute and 0.55 minute for 0.030 inch I.D. Pitot tube and 0.0215 inch I.D. Pitot tube respectively at a given velocity of 1.55 fps. The variation in capillary rise in each tube was investigated by a capillary rise calibration device which consisted of a seven inch O.D. vessel, elevation scale, Y type branches and rubber tubes. The results were shown in Fig. 14. Five mm glass tube had a small variation of capillary rise with 3.4 per cent ratio of the change of capillary rise to the original capillary rise, compared to 12.6 per cent by capillary tube, and to 16.7 per cent by seven mm glass tube. Twelve mm glass tube had a better effect in capillary rise but its extremely long time lag did not admit it for the use as the manometer.

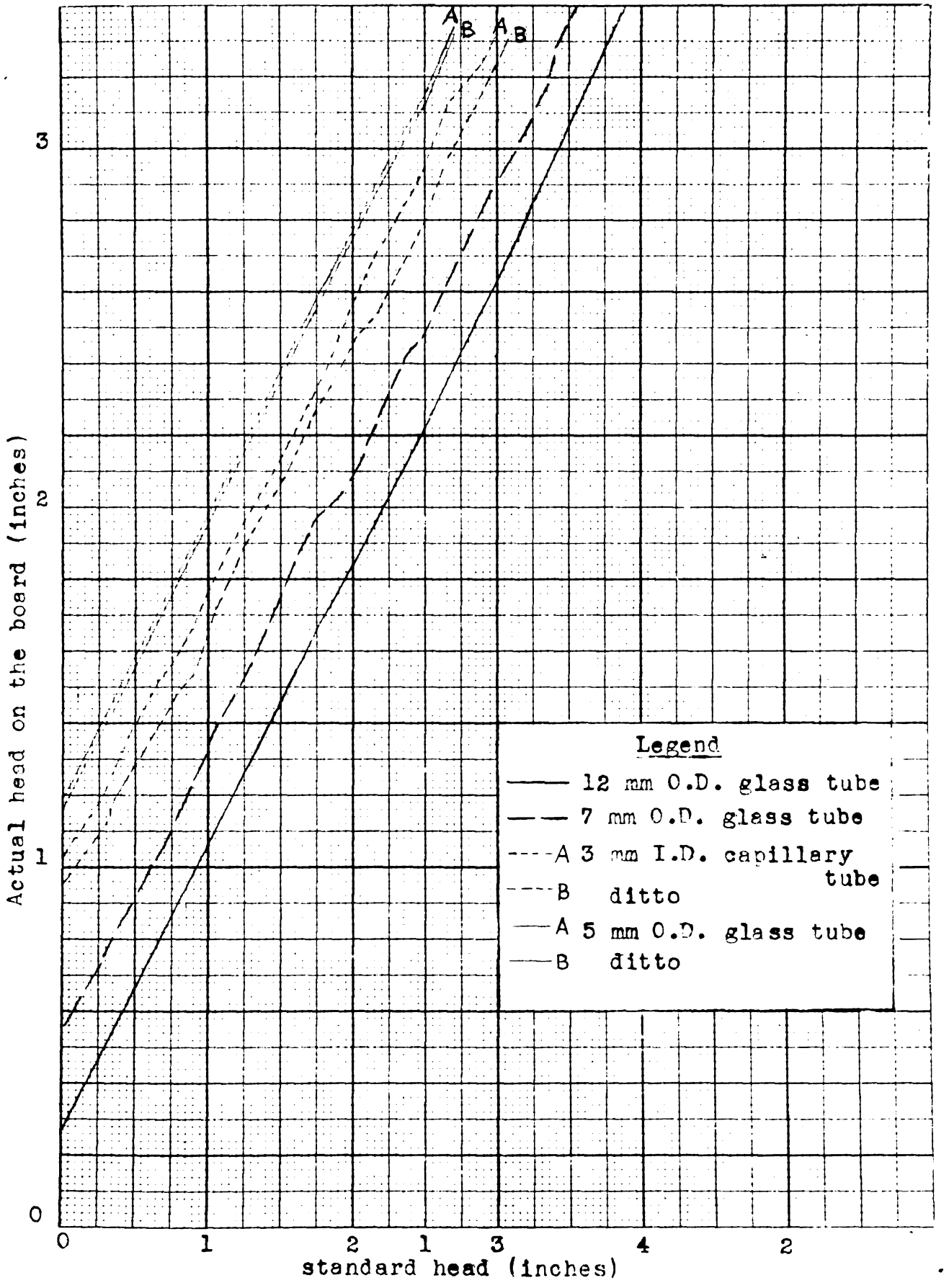

Fig. 14. Variation of capillary rises in four manometer tube sizes on 30 degree inclined board.

Five mm glass tube was selected as an ideal size of manometer tube for this study on account of acceptable time lag and controlled capillary effect.

The approximate variation of tube diameter in five mm glass tube was computed from formula (6) as about 0.1 per cent of the ratio of change of diameter to the original tube diameter. It was determined that the use of five mm glass tube for measuring velocity or pressure head in this study, would result in one or two minutes time lag and about three per cent variation of capillary effect, which was compensated by the calibration of manometer board on account of different capillary effect at each elevation due to the change of inside diameter of the tube.

E. A Chemical Treatment for the Dissipation of Surface Tension.

Due to the surface tensions of water, capillary rise caused a meniscus in the tube. In order to dissipate the meniscus or retard the capillary effect, several chemicals were tried in this study. When these chemicals were added on the meniscus in the manometer tube the resulting surface tension was about seven to ten times lower than for the water alone. From formula (20)

$$\Delta d = \frac{\Delta h d^2}{C - \Delta h d} \qquad \therefore \Delta h = C \frac{\Delta d}{d(d-\Delta d)}$$

$$\therefore C = \frac{4\sigma \cos\beta}{\gamma}$$

If $\frac{\Delta d}{d(d-\Delta d)}$ is fixed and C will be variable due to the change of surface tension, σ, then σ and C have a proportional relation when contact angle of water and tube wall, β, and specific weight, γ, are assumed to be constant. Therefore Δh has a proportional relation with σ. If

$$\frac{4 \cos\beta \, \Delta d}{\gamma d(d-\Delta d)} = K \quad \text{(constant)}$$

$$\Delta h = \sigma K \qquad (21)$$

If σ decreases Δh will proportionally decrease. So in this study, an attempt to eliminate or decrease the variance of capillary rises in the same size manometer tube due to the slight change in diameter of the same size tubes, was carried out. The surface tensions at the interface between two liquids, so-called interfacial tensions, (each liquid saturated with the other) were referred to Handbook of Chemistry and Physics (P.1869 34th Edition Chemical Rubber Publishing Co.) as follows:

at 20°C temperature

between:	(dyn/cm)	(lbs/ft)
water-Ethyl ether	10.7	0.000733
water-Heptylic acid	7.0	0.00048
water-Octyl alcohol	8.5	0.000583
water-air	72.75	0.00499

The data shows that there is about seven times more surface tension in water-air than in water-Ethyl ether, and ten times more in water-air than in water-Heptylic acid. The term Δh will decrease ten times as the σ decrease ten times according to the assumption on which equation (21) is based. Therefore the variation of capillary rises was supposed to be eliminated. In the experiment, Ethyl ether and n-Valeric acid respectively were tried, and which was found quite effective in application to the same size tubes.

It was difficult, however, to supply the same vertical height of chemical to each tube so that the increment in pressure head on each water column would be the same.

Actually it was a complicated process to eliminate the variation of capillary rise by this method, when compared to the direct calibration method.

For the sake of efficiency, it was believed that the direct calibration method for capillary rise at each elevation was a more effective method.

The reason for using n-Valeric acid instead of Hyptylic acid was that n-Valeric acid has similar property in the as-

pect of carbon number; n-Valeric acid has five carbons while Hyptylic acid has seven, and which means it was insoluble in water due to the high number of carbons.

Fig. 15 demonstrated the result of adding n-Valeric acid to the top surface of water column in the manometer tubes. There was an apparent effect on the interfacial tension between water and the acid.

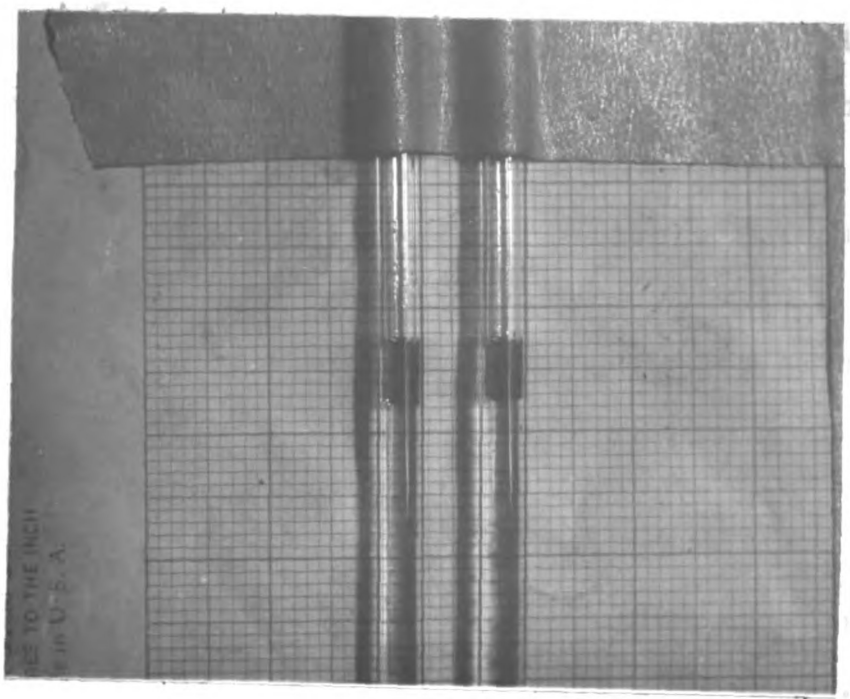

Fig. 15. View of the effect of chemical treatment on the capillary rises.

F. Description of Constructed Manometers

Vertical board manometer: Four 5 mm regular soft glass tubes four feet long each, were placed on the vertical board. Graph strips, 20 squares to the inch were used as the scale. (Fig. 12) The actual calibration was completed on the scale in order to eliminate error from capillary rise due to variation of diameter of the tube. A part of the calibrated board scale is shown in Fig. 16. These scales were used with piezometer tube for measurement of static pressure at the plastic tube wall, also occasionally for higher velocity head measurement.

Thirty degree inclined board manometer: Eight 5 mm regular soft glass tubes one foot long were provided on the board with 20 squares to the inch graph strips. The scales were calibrated to compensate for capillary effect and bore variation. (Fig. 17) Also two 5 mm double-column manometers, or U-tubes containing mercury with calibrated scale aside, were set on the same board, for the measurement of high velocity head which has fluctuating reading because of the turbulent condition. In this study, the high velocity ranged from four to eight fps.

The eight piezometer tubes were used for lower velocity head measurement.

In order to eliminate or damp out fluctuation of the head reading under turbulent conditions, mercury was used as capacity damping, 1 mm capillary tube and screw clamp were applied

as resistance damping. Careful operation of damping device was necessary to eliminate error.

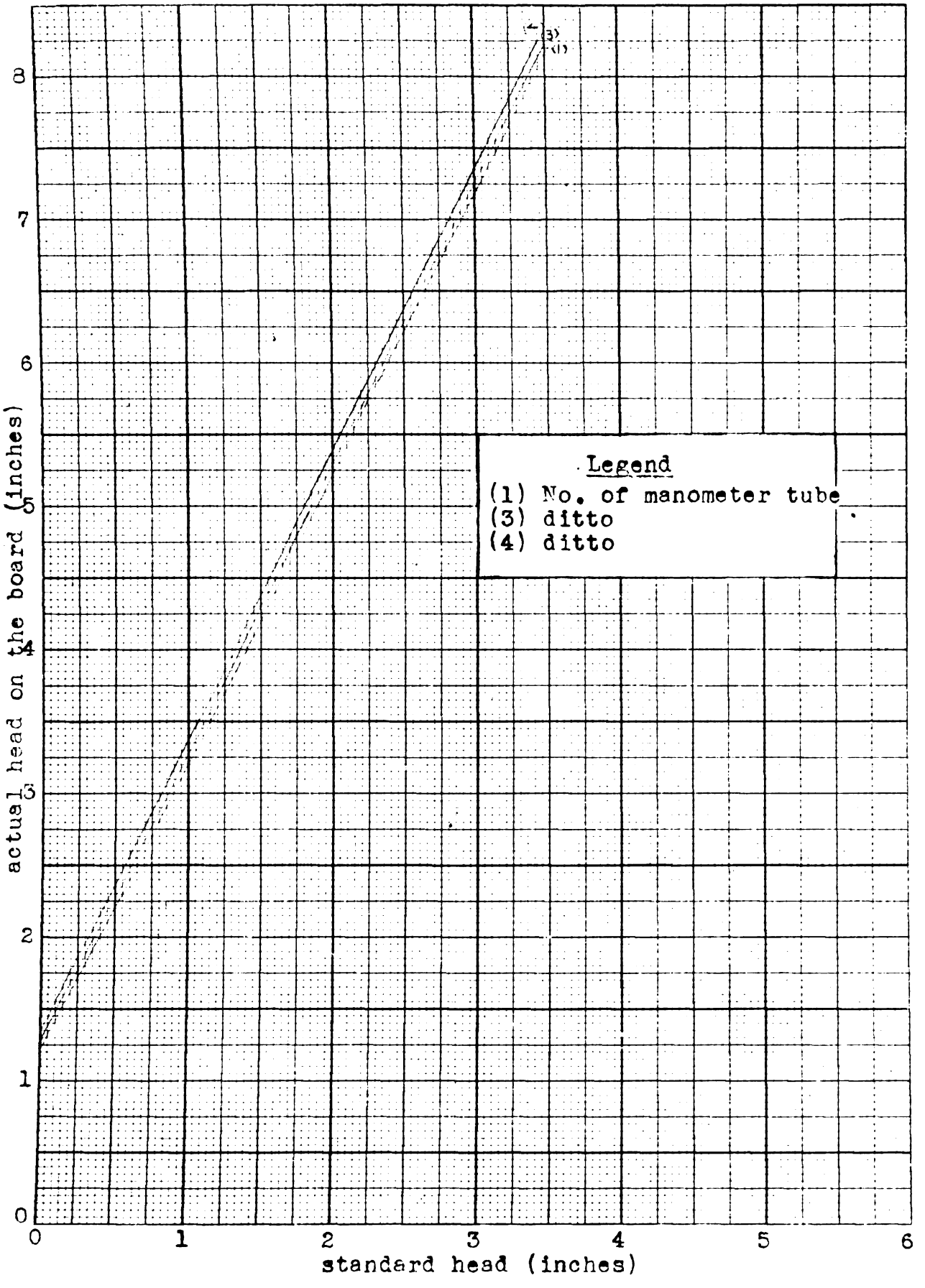

Fig. 16. A part of calibrated 30 degree inclined manometer scale.

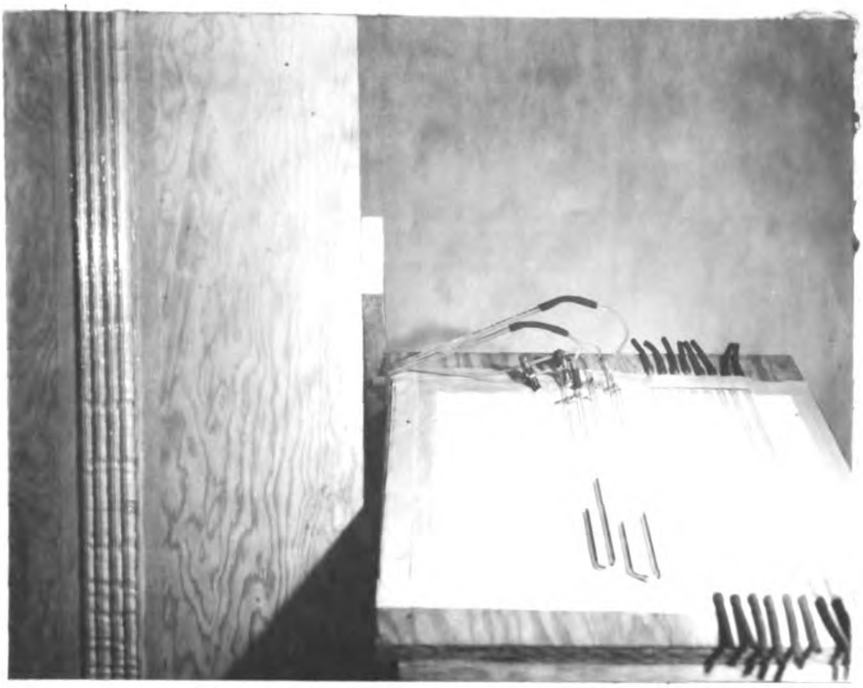

Figure 17. View of 30 degree inclined manometer and vertical manometer.

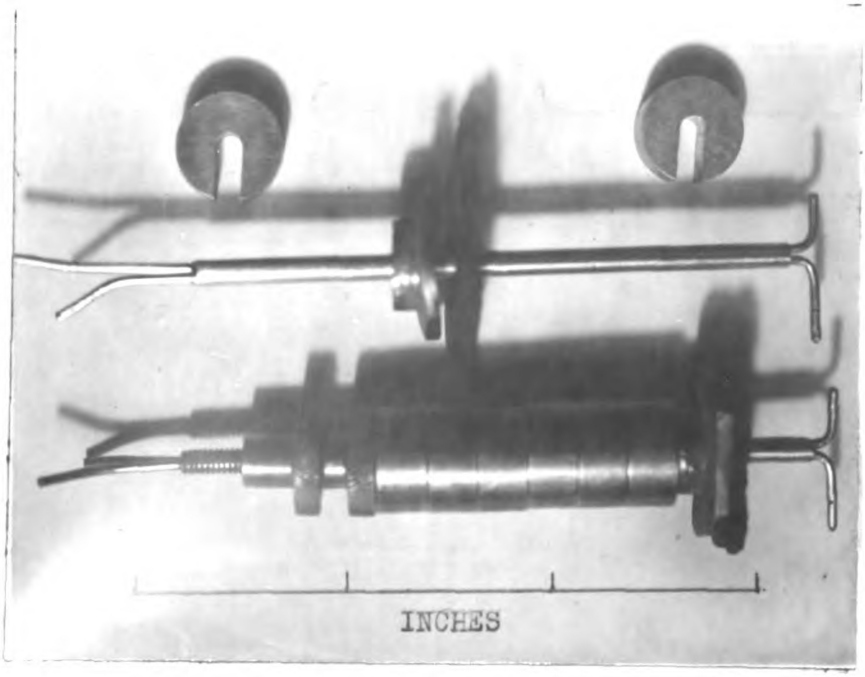

Figure 18. View of constructed Pitot-static tube with double lock nuts and washers.

PITOT TUBE PRACTICE

I. INTRODUCTION

The Pitot tube was considered as a basic instrument for the measurement of velocity distribution in a conduit bend, however, there were some difficulties in measuring two and three dimensional flow. At sections far beyond the bend, the pitot tube is effective in the velocity measurement with a high accuracy, therefore Pitot tube practice was undertaken primarily as a method to approach the study of secondary flow in the bend. The first description of a tube used to measure pressures for velocity determinations was presented by Henri Pitot in 1732. [6]

The name "Pitot tube" has been applied to two general classifications of instruments, the first being a tube that measures the impact or total pressure only, and the second a combined tube that measures both the impact and the static pressure with a single primary instrument.

In order to avoid confusion it is desirable to distinguish between the two types of Pitot tubes: "Pitot tube" and "Pitot-static tube". The Pitot tube consisted of one forward-facing tube to read the dynamic head plus the static head in order to determine the velocity in a closed conduit. A single tube used to measure static pressure was named "static tube". The Pitot-static tube was made up of two tubes: one

reading the dynamic head, the other the static head. (Fig. 18)

The fundamental form of basic equation that applies to Pitot tube or Pitot-static tube measurement is:

$$V = C\sqrt{2gh} \qquad (8)$$

where C is an empirical coefficient depending on the shape of the orifice and on other variables, h is the height of water column in the manometer tube that the velocity V may be determined, and g is the gravitational acceleration.

Before the Pitot tube can be used the value of the coefficient C in the equation (8) should be accurately determined. To do this the instrument must be rated or calibrated by a flow system with several known flow velocities, or it must be towed at various known speeds through still water in a rating channel and the corresponding differential heads noted.

In this study flow system No. 2 was used for the determination of coefficient, C.

In general, the value of C will always be less than unity, because the static tube records a pressure slightly less than the true static pressure, owing to the increase in velocity past the tube. However, for most engineering problems the value of C may be taken as 1.00 for the conventional types of Pitot-static tubes: such as those made by American Blower Company, Prandtl (Gottingen), National Physical Laboratory (England), and American Society of Heating and Ventilating Engineers.

In this study, the relationship between the coefficient, C and the velocity, V was necessary in order to estimate the accuracy of velocity measurement. It was known that this type of Pitot-static tube, similar to the Cole pitometer, had a distinct character that C and V were related almost inverse-proportionally.

II. LITERATURE REVIEW

Broad information about the Pitot tube was obtained from Folsom's [6] "Review of the Pitot Tube".

A. Tube shape

Impact total pressure: The results obtained by a large number of investigators have demonstrated that if the shape of the Pitot head is one in which a stagnation point exists in the flow system, the full impact pressure is measured at a tap located at the stagnation point in uniform velocity flow.

Merriam and Spaulding [11] have investigated the effect of the size of the pressure with respect to the diameter of the Pitot head in the case of a hemispherical tip within the range of $0.2 < \frac{d.}{D} < 0.74$ and found that the size of the hole has no effect on the magnitude of the impact pressure measured at zero yaw. On the other hand, to obtain the true impact pressure, the problem of alignment in yaw of the Pitot head is most critical in the case of the smaller pressure-tap sizes.

Static pressure: When a Pitot tube is used in a pipe and the static pressure is determined by a pipewall piezometer, the pressure distribution about the Pitot tube stem may affect the piezometer pressure. When the head of the Pitot tube extends into the region of the plane of a pipe-wall piezometer, the pressure measured by piezometer tends to be low due to the

reduced cross section of flow.

With a Pitot-static tube or combined tube, the magnitude of pressure sensed at the static-pressure tap may be a function of the shape of the tip and the distance from the tip to the plane of the holes.

Hemoke's test (6) demonstrated that hole diameters of the piezometer must be less than about 0.06 inch for accurate pressure-distribution measurements. The pressures on the rear side of the cylinder were independent of hole size.

B. Fluid-flow characteristics

Turbulence: Turbulence in the fluid stream may have a decided effect on the flow in a system, such as changing the boundary layer characteristics, including the separation point, and producing a pressure reading on a Pitot-static higher than the true mean pressure. On the basis of the theory of isotropic turbulence, Goldstein (9) obtains the expressions for the pressures as

$$\text{total head} = P + \frac{\rho V^2}{2} + \frac{\overline{\rho(v')^2}}{2}$$

$$\text{static pressure} = P_s + \frac{\overline{\rho(v')^2}}{6}$$

where is the resultant mean velocity and the resultant turbulent velocity. Flow in pipe does not exhibit isotropic turbulence, and Fage calculated on the basis of turbulence measurements.

$$\text{static pressure} = P_s + \frac{\overline{\rho(v')^2}}{4}$$

For the usual degree of turbulence at sections in pipes of fully developed velocity distribution, the turbulence errors

are small and tend to equalize in the velocity determination. For higher degrees of turbulence it is possible for the turbulence errors to reach appreciable magnitudes in terms of dynamic pressure.

C. Dynamical similarity

Reynolds Number: A wide range of experiments has shown no change in Pitot tube pressure-coefficient characteristics at values of Re greater than about 500 and for Pitot-static probes (NPL type) at values of Re greater than about 2300 with Re based on probe-head external diameter. At Re = 500 pressure coefficient $C_1 = \frac{P_i - P_\infty}{\frac{\rho V_\infty^2}{2}}$ is increasingly greater than unity as the Re decreases, actually values depending on the geometry of the probe and impact opening.

Mutual interference: When pressure-measuring tubes are placed in the vicinity of fluid boundary, the tube calibrations made without such boundary usually can not be applied directly.

Comparisons of hot-wire and impact tube with known static pressure for velocity measurement in the boundary layer have shown good correlation as long as the tube diameter is small enough. Care must be exercised when making measurements in the flow passages of turbomachines for the purpose of interpreting the instrument readings obtained.

Comparative tests of Pitot-static tubes by Merrian and Spaulding [11] have demonstrated that the effect of 15 yaw degrees resulted in a five per cent error; 24 yaw degrees

- 13 per cent error in decrease of pressure head. The effect of static openings on static-pressure error was shown as follows: when diameter of static opening was 0.02 inch and degree of yaw was zero degree, the error became 0.05 per cent, at eight degrees of yaw the error was 1.1 per cent. Thus it was found there was the same percentage error on the two diameters of opening for static pressure. The difference in total pressure heads resulting from round connection and square connection was investigated and found to be 0.3 per cent when the distance between the tip and the vertical stem was five times the diameter of the Pitot tube and 0.05 per cent for 10 diameter distance. Chesky, Hurd and Shapiro [7] found that above Reynolds number of 1000, there is no effect of viscosity, and the pressure coefficient, Cp is equal to unity. Between Re $\cong$ 50 and Re $\cong$ 1000, Cp is always greater than unity. When Re is below unity, the pressure rise is independent of the fluid density, and the data may be approximately represented by the formula $Cp \cong \frac{5.6}{Re}$

$$Cp \equiv \frac{2\Delta P}{\rho V_\infty^2}$$

Δp is the excess of stagnation-point pressure over free-stream static pressure, V is the free-stream velocity, ρ is the fluid density.

Goldstein [9] mentioned that usually a small diameter of single Pitot tube is required for detailed explorations of the flow in the boundary layers of bodies such as cylinders of stream line solids of revolution, and in traverse sections

of pipes, and the only limitation to be observed in this respect is that Barker's criterion, $\frac{Vd}{\nu} > 30$ is still fulfilled at the lowest velocity it is proposed to measure in any particular case. The tubes are best operated by means of a micrometer arrangement.

Cole [15] discussed the practical application of the Pitot tube to flow measurement, corrections for the effect of the projected area of the rod, and the errors caused by angularity of flow in a pipe. He also presented the following items: (a) a suitable means for inserting the tube into the pipe under pressure. (b) a practical and accurate method for calibrating the instrument, (c) a differential manometer free from air which contains a liquid permitting the magnification of the deflections at low velocities, and (e) a means for the frictionless recording of manometer deflection where a continuous record of flow is necessary. In connection with calibration, the following items must be considered: (1) For important tests the tube must be calibrated. (2) Proper correction must be made for the effect of the projected area of the rod. (3) The effect of angular and eddying flow in the normal pipe line may be corrected by a cosine-reading type of tube.

The following details of operation which comprise the Pitot-traverse method are also important: (a) A proper selection of gauging point must be made. (b) The pipe factor, i.e. ratio of mean to center velocity, is of fundamental value and is determined by traversing the pipe. The

mean velocity of the traverse is obtained by ring integration, and the value for the center velocities taken from the traverse curve. (c) All readings of the deflection should be made through out a full cycle of flow and careful attention given to the U-tube and its connections, and the specific gravity of the measuring liquid. (d) For large pipe, attention should be given to the possible effect of vibration of the Pitot tube.

In Coles' test at the Alden Hydraulic Laboratory, Worcester Polytechnic Institute in 1930-1934, seven different Pitot tubes (Cole Pitometer) were tested both in moving water and still water. The results are shown in Fig. 20, in which the indication led the author to believe that with the proper correction for the projected area of the rod, when used in pipes, calibrations by either of two methods will give the same results.

A summary of previous Pitot tube calibration data compiled by Cole indicated that single Pitot tubes had coefficients of unity, and most Pitot tubes or combined Pitot tubes had coefficient of less than unity.

III. DEVELOPMENT OF PITOT-STATIC TUBE

A. Determination of the Size of Pitot-static Tube

The size of Pitot-static tube suitable for this study was determined. The following four sizes of Pitot tube and four sizes of static tube were evaluated in this test:

(1) 0.060 inch I.D. Pitot tube or static tube.

(2) 0.045 inch I.D. Pitot tube or static tube.

(3) 0.030 inch I.D. Pitot tube or static tube.

(4) 0.0215 inch I.D. Pitot tube or static tube.

The four different sizes of Pitot tube (total pressure tube) and static tube (static or piezometric pressure tube) as shown in Fig. 13, were inserted into the section of flow system No. 1, extended fifteen diameters of length downstream from the bend in the two inch plastic tube. The Pitot tubes or static tubes were convergently moved from four directions to the center of the section where the velocity of flow was assumed to be approximately the same within certain cross-sectional area around the center. Therefore the four Pitot tubes or static tubes were considered to receive the same amount of dynamic or static pressure respectively in the water flow.

Total or static pressure heads received respectively by four single Pitot tubes and four static tubes, were measured by thirty degree inclined manometer (piezometer tubes) at the velocities ranged from 0.75 to 2.90 fps. The results shown in Fig. 19 express the variation of pressure head due to the

size of Pitot tube and velocity of water flow in the plastic tube, while the viscosity of water was assumed to be constant. In this test, the space between the four Pitot tubes or static tubes converging to the center of the section, were kept at about 0.1 inch between each two tubes in the final position in order to avoid the influence of boundary effect of each tip of a tube on adjacent tubes.

From experimental results shown in Fig. 19, it was demonstrated that pressure coefficients, C_p, of the four Pitot tubes were unity at the velocity higher than 0.75 fps, but there was a small variation of pressure coefficient, C_p, at the velocity 0.75 fps. Referring to Barker [9] [7], Homann and Hurd [7], C_p, was defined as the ratio of measured velocity head to the given velocity head at the stagnation-point on the tip of the Pitot tube. For values of Reynold's number, Re, less than 50, it was determined that C_p is always greater than unity.

While in this test, 0.0215 inch single Pitot tube with 0.75 fps velocity had a Re of 49.2, ($Re = \frac{Va}{\nu}$ where V = velocity in the tube, a = radius of the tube, ν = kinematic viscosity; according to British reference) and for 0.030 inch single Pitot tube the Re was 70. According to reference [7] and [9] which demonstrated the pressure coefficient as a function of Reynolds number, there was some doubt about the unity of pressure coefficient, C_p, at the velocity of 0.75 fps for 0.0215 inch Pitot tube.

At the velocity of 2.95 fps, slight variation of pressure

head in the four different sizes of Pitot tubes and static tubes occurred due to the pressure fluctuation in the flow system No. 1.

As for static pressure heads recorded by four static tubes respectively in Fig. 19 at the velocities ranging from 0.75 to 2.90 fps, it was found that there was some irregular variation of C_p in the four sizes of static tube through the range of velocity, because of a complicated boundary layer effect and suction effect due to the size of the piezometer hole compared to the size of the Pitot tube. No reference was found on this aspect concerning the static pressure coefficient as a function of Reynolds number. It was concluded that the ideal size of Pitot-static tube for the velocity measurement in further study is 0.030 inch I.D. for the following three reasons:

(1) high efficiency in velocity measurement because of its greater dynamic response to the flow, compared to 0.0215 inch I.D. Pitot tube.

(2) a confirmation of the unity pressure coefficient for the Pitot tube at the velocity higher than 0.8 fps (Re $\pm$70)

(3) the effective area of the 0.030 inch I.D. Pitot-static tube orifice is regarded as geometric point, comparing to the total cross-sectional area of plastic tube.

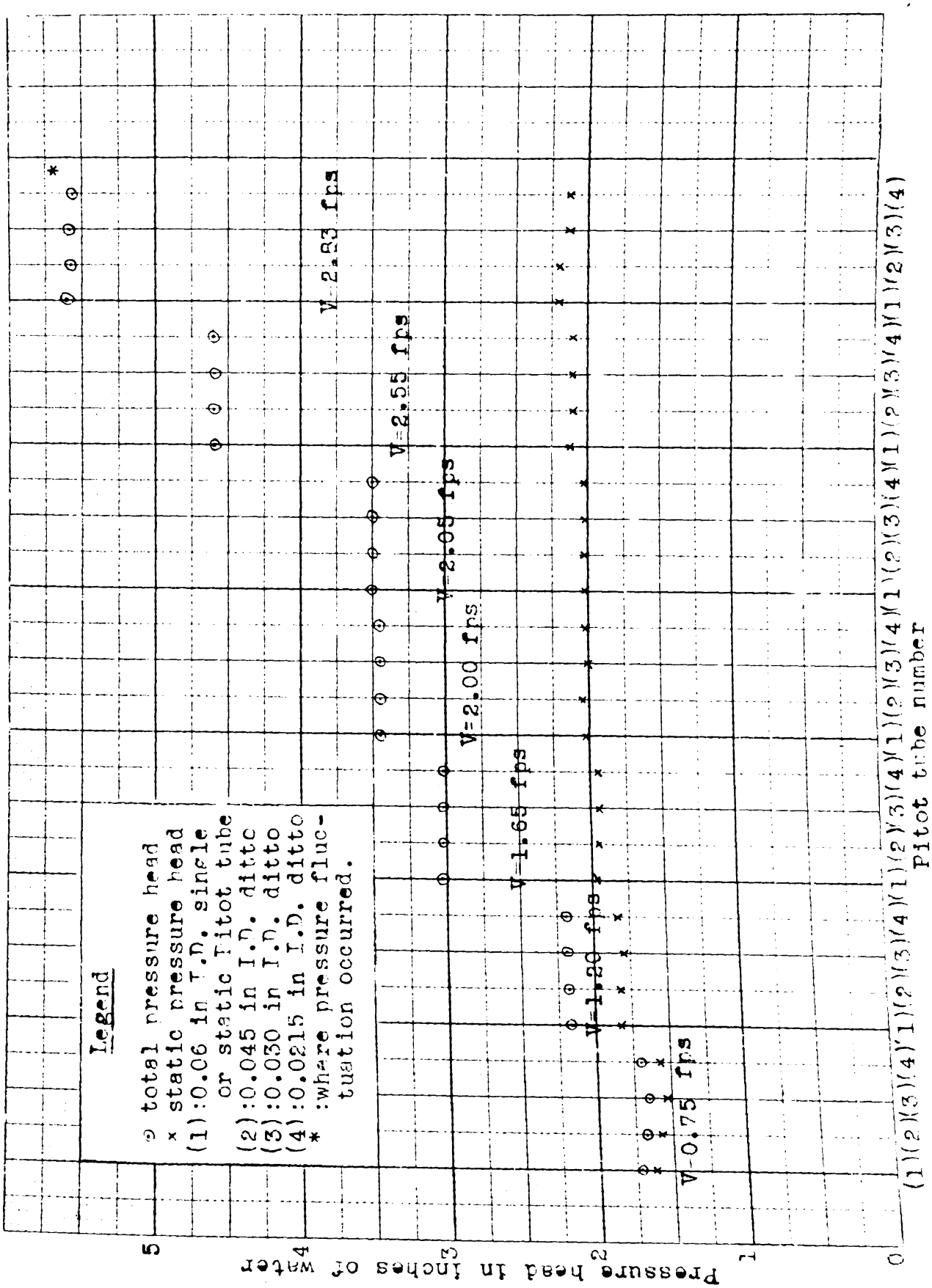

Fig. 19. Results of the test for viscosity effect on four Pitot tube sizes.

B. Construction of Pitot-static tube

After determining that the 0.030 inch I.D. hypodermic needle was the proper size for the Pitot-static tube in this study, the technical reports of the Pitot-static tube by Merrian & Spaulding [11], Folsom [6], Hurd [7], Goldstein [9], Cole [5], and Addison [2] were studied. The following specific information was obtained as reference for the construction of the Pitot-static tube:

1. 0.02 inch diameter static opening or piezometer hole resulted in 0.05 per cent static pressure error, while the 0.04 inch had 0.05 per cent error, referring to Merriam & Spaulding's experimental results. [11]

2. The differential error of total pressure between using round connection Pitot tube and square connection Pitot tube, was 0.05 per cent when the tip was at ten diameters of Pitot tube distance from the connection or the bend: five diameters distance had 0.3 per cent error (From Merriam & Spaulding reports. [11]

3. Value of the coefficient, C, in velocity formula $V = C\sqrt{2gh}$, will depend on the form of the instrument, on the turbulence in the stream, and on the Reynolds number of the flow past the tube. (From Goldstein [9])

4. The influence of impact-tube size (or Pitot tube size) in a uniform-velocity stream was checked by Zahm [6], using a 1/8 inch diameter square ended tube against a five inch diameter pipe as well as a 1/8 inch glass tube against

a 0.01 inch I.D. hypodermic needle. Both checks gave the same impact pressure within instrumentation tolerance.

5. In Pitot tube made by Cole, (so-called Pitometer) the tube facing downstream measures the pressure in the turbulent wake behind itself, which is less than the true static pressure. The coefficient of the Pitometer is, therefore, much less than unity. (5)

The 0.030 inch I.D. Pitot-static tube was designed and constructed similar to a Cole pitometer after giving consideration to the above information, with a difference that the static pressure was measured at the static opening or piezometer hole on the static tube facing downstream, instead of at the end of the tube. (Fig. 13) A minimum radius 90 degree elbow connection was made between the tip section and the stem at a point ten diameters of Pitot tube distance from the orifice of the tip. The cross-section at the 90 degree elbow was kept as large as possible.

In the static tube, the distance from orifice of the tip to the elbow connection was 15 diameters of the tube, and the orifice was filled with solder. Three 0.020 inch diameter static openings were located on the wall of the tip, around the section five diameters distance from the orifice of the tip. The minimum radius elbow of the Pitot-static tube made it possible to measure the velocity in the boundary layer close to the inside wall of the plastic tube. The Pitot tube and static tube were inserted into the inside of 1/8 inch O.D.

(0.10 inch I.D.) hypodermic needle, 2.5 inches long. The two tips were faced in opposite directions to each other as shown in Fig. 13 and 18.

In order to decrease the turbulent wake effect on the static tube with the 1/8 inch O.D. stem, the covering tube was kept at a distance 1/8 inch from the tip of the Pitot-static tube. (Fig. 18)

The Brass Collar:

The constructed Pitot tube was mounted in a 3/16 inch thick brass collar, and was located on the wall of the plastic tube with a rubber seal which was cemented between the brass collar and the outside wall of the tube.

Two Positioning Devices:

The first positioning device for the Pitot-static tube when traversing the plastic tube section, was supplied with double lock nuts and eight 0.23 inch equal thickness brass washers. The washers were inserted between the lock nuts fastened on the Pitot tube and the brass collar in order to provide a definite position for the Pitot-static tube in velocity traverse measurements.

The second device consisted of making eight equally spaced marks on the outside wall of the Pitot-static tube stem. The outside surface of the brass collar was used as the reference point to determine the position of the Pitot orifice. (Fig. 18) From the experimental results, it was noted that the effects of the two positioning devices on the measurement of velocity distribution were identical. Four

similar types of Pitot-static tubes were constructed in this study.

C. Correction for Projected Area of Rod.

According to the continuity equation, $Q = VA = \text{constant}$, either the change of velocity or cross-sectional area in a constant fluid flow, may affect the other element in an inverse proportional manner. The insertion of a 1/8 inch effective diameter Pitot-static tube into the two inch I.D. plastic tube section reduces the plastic tube cross sectional area by an amount equal to the full area of the stem. Thus the mean velocity by that section is increased above the value when the Pitot tube was not present.

From the previous study by Cole and Pardoe [5] and the experimental results in this study, it was believed that the upstream orifice of the Pitot tube for total pressure measurement was not affected by the stem effect which decreasing or increasing the cross-sectional area within the plastic tube, and since the most effects of turbulent wake and velocity change due to the reduction of the cross-section were affected on the static tube. Because of this reduction of the cross section, the shape of the traverse curve of velocity measurement was apparently distorted, the measured velocities being higher on the far side of the plastic tube than the value when there was not appreciable reduction of cross section by the traversing Pitot tube stem. In small tubes or pipes the effect of this reduction in the flow section is serious. However, the variation in the velocity distribution across the section due to the reduction effect, was difficult to

investigate. Nevertheless, it was assumed that the ratio of the point velocity to mean velocity remains constant.

Apparatus: Flow system No. 2 was applied in this test. The flow was well regulated within 0.5 per cent variation of discharge rate of flow. A centrifugal pump discharged water into the tanks with an overflow to maintain an essentially constant head. During the Pitot-static tube traverse test, continuous weighing tank measurements were made to determine the true mean velocity. The three orifices provided in the vertical wall of the tank made possible flow velocities ranging from six to eight fps.

Pitot-static tube gaging sections in the four foot length of plastic straight tube, were located at 10, 15, and 19 tube diameters distances from the tube inlet respectively. In each gaging section eight equally spaced Pitot-static tube openings were made in the circumference of the tube, the zero location was at the top or vertical position. In some tests one of the four Pitot tubes was inserted from one of the four axis such as the vertical, the horizontal, and at 45 degrees diagonals. At the same time a dummy stem of the same size as the Pitot-static tube stem was inserted from the opposite direction in the tube section, and the two were moved simultaneously as a pair or as one continuous stem in the tube. A 0.1 inch constant spacing was maintained between the two opposite stems. The purpose of passing the dummy stem with the Pitot-static tube was to maintain a constant reduction in the plastic tube cross-section when the

Pitot-static tube was in use. A rubber seal cemented between the brass collar and the tube wall prevented water leakage. Two Pitot-static tubes were also inserted from opposite directions along the vertical, or horizontal or diagonal axis at the section, and were moved simultaneously as a pair with 0.1 inch spacing between the two opposite Pitot-static tubes at all times.

The mounted Pitot-static tubes were connected by 0.06 inch I.D. flexible plastic tube to the mercury manometers or piezometer tubes. The static pressures were measured at the points one diameter upstream and downstream from the gaging section.

Procedures in the Test: Two methods of correction with a checking procedure were tested. They are:

a) Single traversing method with correction ratio: The method was to locate a Pitot-static tube as a gaging stem at some point in the plastic tube and without changing its position to move a second or dummy (may be called pilot rod) Pitot-static tube across the plastic tube on another diameter in the same gaging section. The location of the orifice of gaging stem was defined at 0.015 inch (in this case, actually, Pitot-static tube tip was contacted to the wall of the tube), 0.115 inch, 0.462 inch and 0.90 inch respectively from inside wall of the plastic tube from which it was inserted.

It was indicated by the first Pitot-static tube, that the further the dummy stem was projected, the greater would

be the velocity indicated by the gaging stem. It was apparent that the dummy stem would disturb the flow past the gaging stem if it were too close, and various positions of the indicating stem were tried to note the effect of disturbance.

The experimental results were shown in Fig. 21, where the correction curves were drawn with the ratio of original velocity head measured gaging stem when the dummy stem was not present, to the velocity head measured by index stem when the dummy stem was traversing into the tube to any location, as the ordinate, and the change in ratio of areas as the abscissa. It was noted in Fig. 21 that each Pitot-static tube had a different slope of curve, expressing its different response to the effect of disturbance.

The locations of the nine traversing positions in the section for dummy stem were uniformly distributed through the diameter, i.e. eight equally divided spaces. The mean velocities applied for correction curves, varied from 6.86 to 7.50 fps.

These curves in Fig. 21 were applied for the compensation of distortion on the velocity distribution curves measured by the four Pitot-static tubes respectively.

In the correction, two systems were applied; the one placed the initial correction point on the traverse point number one, then the correction ratio increased from zero at the entry side of the tube wall to a maximum correction at the far side of the wall; the second method placed the initial correction point at the center, thus there would be a plus correction on one side,

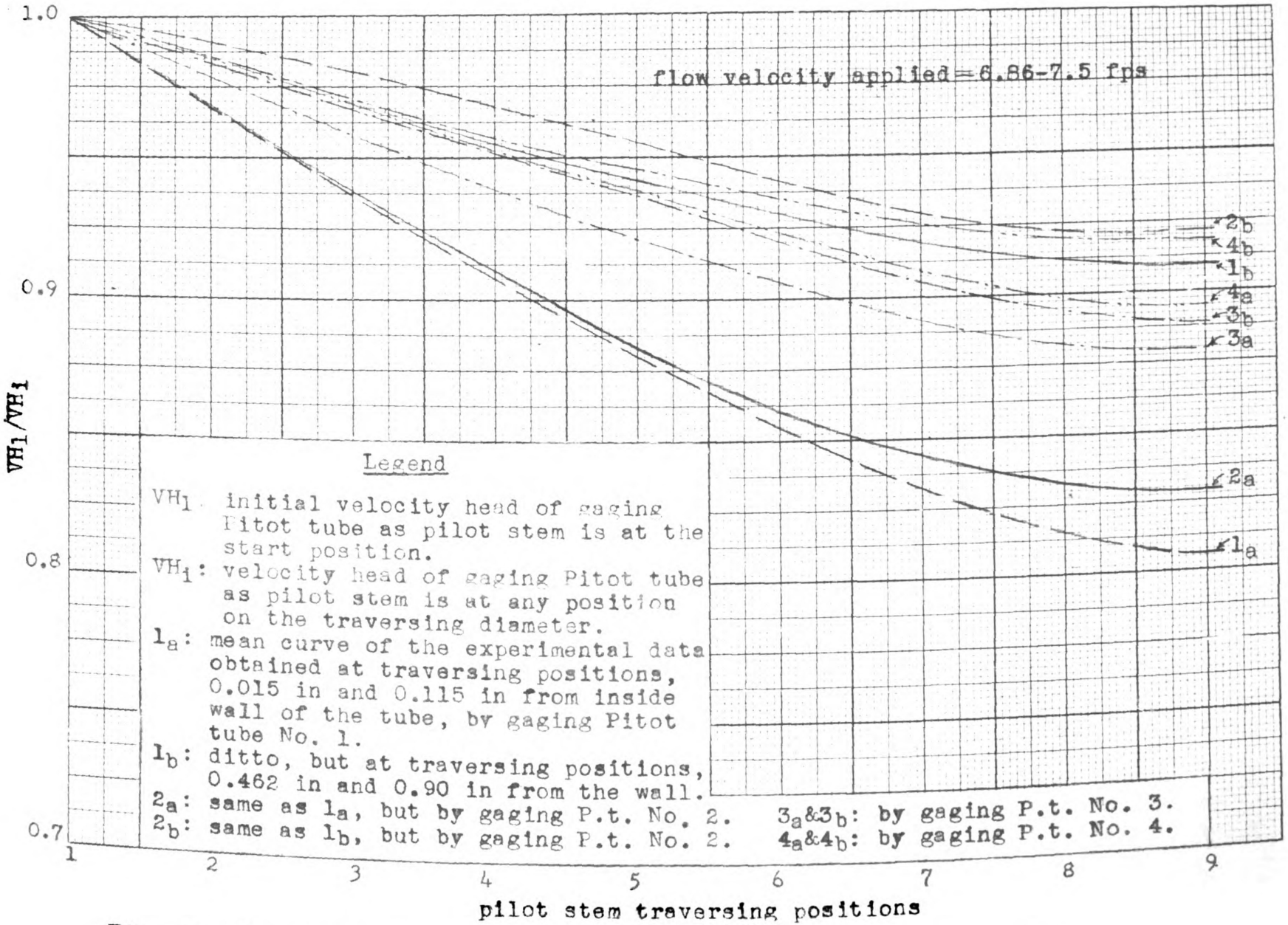

Fig. 21. Correction curves for Pitot tube single traversing method.

assuming the readings are to be corrected with respect to the Pitot tube at the center. One of the corrected velocity distribution curves and the original curves drawn by single traversing method with correction ratio are shown in Fig. 22.

b) Double traversing method with correction ratio: In order to eliminate the effect of area reduction causing a distortion of the velocity distribution curve, the direct method was applied instead of depending on the corrective curves. The four Pitot-static tubes were inserted from opposite directions along the vertical and horizontal axis, and 45 degree diagonal axis. However, only one pair, two directly opposite each other, were used at one time. These Pitot-static tubes were moved simultaneously through the diameter with 0.1 inch spacing constantly maintained between the two opposite Pitot-static tubes. Readings were simultaneously taken from both Pitot-static tubes at each traversing point. The velocity distribution curves measured with four Pitot-static tubes respectively, at each gaging section along the four axes, were drawn as the one shown in Fig. 25. The correction to the velocity distribution curve was made by abstraction of the velocity increment due to the constant projected area, with the assumption that the ratio of mean velocity change determined by weighing-tank measurement, caused by the reduction of tube section might be the same as the ratio of velocity change at any point on the velocity distribution curve during the same test.

If V_a is the mean velocity determined by weighing-tank

meas

effe

dire

tan

A_a

are

dir

The

Ac

if

t

measurement, with plastic tube cross-sectional area minus effective area of double traversing Pitot tube in the flow direction, V is the mean velocity determined by weighing-tank measurement with plastic tube full cross-sectional area, A_a is the plastic tube cross-sectional area minus effective area of double traversing Pitot-static tubes in the flow direction, A is the plastic tube full cross-sectional area. Then if discharge Q is constant: $Q = A_a V_a = AV$

since $A_a \neq A$ $V_a \neq V$

$$\text{if} \quad K = \frac{v}{v_a} = \frac{V}{V_a} \quad \text{uniform}$$

According to an assumption, that, increment exists at velocity distribution curves due to the change of tube cross-sectional area.

$$\text{then } \frac{1}{K} \doteq \frac{A}{A_a}$$

$$\text{thus } v = v_a K = v_a \frac{V}{V_a}$$

Where v_a is the velocity at any point on the velocity distribution curve along the diameter with the plastic tube cross-sectional area minus effective area of the double traversing Pitot-static tubes in the flow direction, v is the velocity at any point on the velocity distribution curve along the diameter of the plastic tube full cross-sectional area. A sample computation for discharge, Q = 0.13223 cfs in two inches O.D. (1.85 I.D.) plastic tube follows:

A_a = 0.017166 ft.^{2}

A = 0.0187 ft.^{2}

V_a = 0.13223 ÷ 0.01766 = 7.7 fps

$V = 0.13223 + 0.0187 = 7.07$ fps

$v_a = 8.45$ fps (measured at the center of the tube)

then $v = v_a \frac{V}{V_a} = 8.45 \times \frac{7.07}{7.7} = 7.76$ fps

One of the experimental results was presented with the above correction method in Fig. 22.

c) Checking procedure: The disturbance caused by the presence of the static tube was eliminated by use of a wall piezometer opening one diameter upstream from the total head tube. The velocity distribution curve was drawn by this measuring method along the diameter by which the results of single and double traversing methods were compared and the reliability on these methods was evaluated.

Moreover by using single and double traversing method for the measurement of total pressure head with the Pitot tube, the effect of stem to the orifice of Pitot tube was examined as shown in Fig. 22. The maximum difference between two methods in velocity measurement was determined as 1.4 per cent.

Discussion of the Experimental Results:

With the exception of two lower correction curves for Pitot-static tube number one and number two respectively in Fig. 21 the other correction curves fall within four per cent of one another, therefore the mean curve may be considered accurate within two per cent for the correction in the single traversing method.

The two traversing methods were compared and evaluated in

Test condition: discharge rate, Q = 0.13283 cfs; gaging station at ten tube dia. distance from tube inlet;
with orifice No. 1; temperature of water = 53 degree F.

with bell-shaped nozzle; with orifice No. 1; temperature of water = 53 degree F.

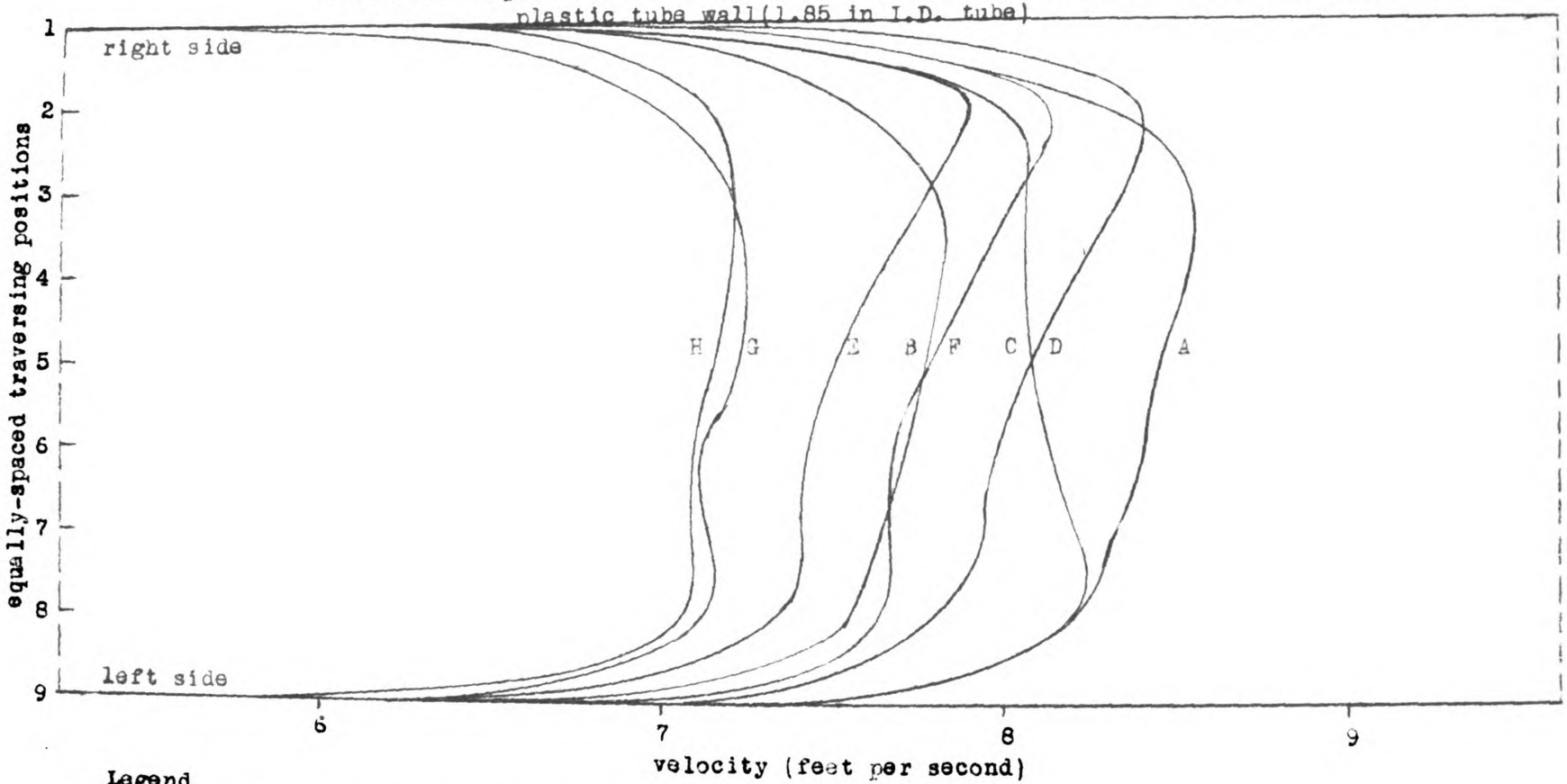

Legend

velocity distribution curves along horizontal axis;
A: by double traversing method without correction.
B: by double traversing method with correction.
C: by single traversing method without correction.
D: by single traversing method with correction started from traversing position No. 5.
E: by single traversing method with correction started from traversing position No. 1.
F: by single traversing method with average correction of curve D and E.
G: by double traversing method with static pressure head measured at tube wall and without correction.
H: bysingle traversing method with static pressure head measured at tube wall and without correction.

Fig. 22. Comparison of the velocity distribution curves measured by various Pitot tube traversing methods.

Fig. 22. It was noted that in the single traversing method, the two systems for correction; with the initial point at the side wall of the plastic tube and at the center (traversing position no. 1 and no. 5), had no significant difference, hence the corrected distribution curves were similar but a difference in the magnitude of velocity caused by half diameter length of projected area for the reduction of tube section.

The double traversing method was successful in bringing out the similarity of the distribution pattern with the reliable distribution pattern as determined by checking procedure. Because of the significant similarity in the two distribution patterns measured by checking procedure with single and double traversing method, it was concluded that there was no apparent effect of the stem on the orifice performance in the single Pitot tube when it is facing the upstream in the tube.

Imperfections of correction ratio to the velocity distribution curve are shown in Fig. 23. Two Pitot-static tubes were alternatively inserted along the horizontal axis into the tube from right and left sides for velocity measurement by single traversing method. The distribution curves along the same axis were adjusted by the correction ratio respectively, and were drawn in Fig. 23, which failed to show the similarity of the two distribution curves measured from both the right and left sides along the horizontal axis.

As a conclusion, it was noted that the double traversing

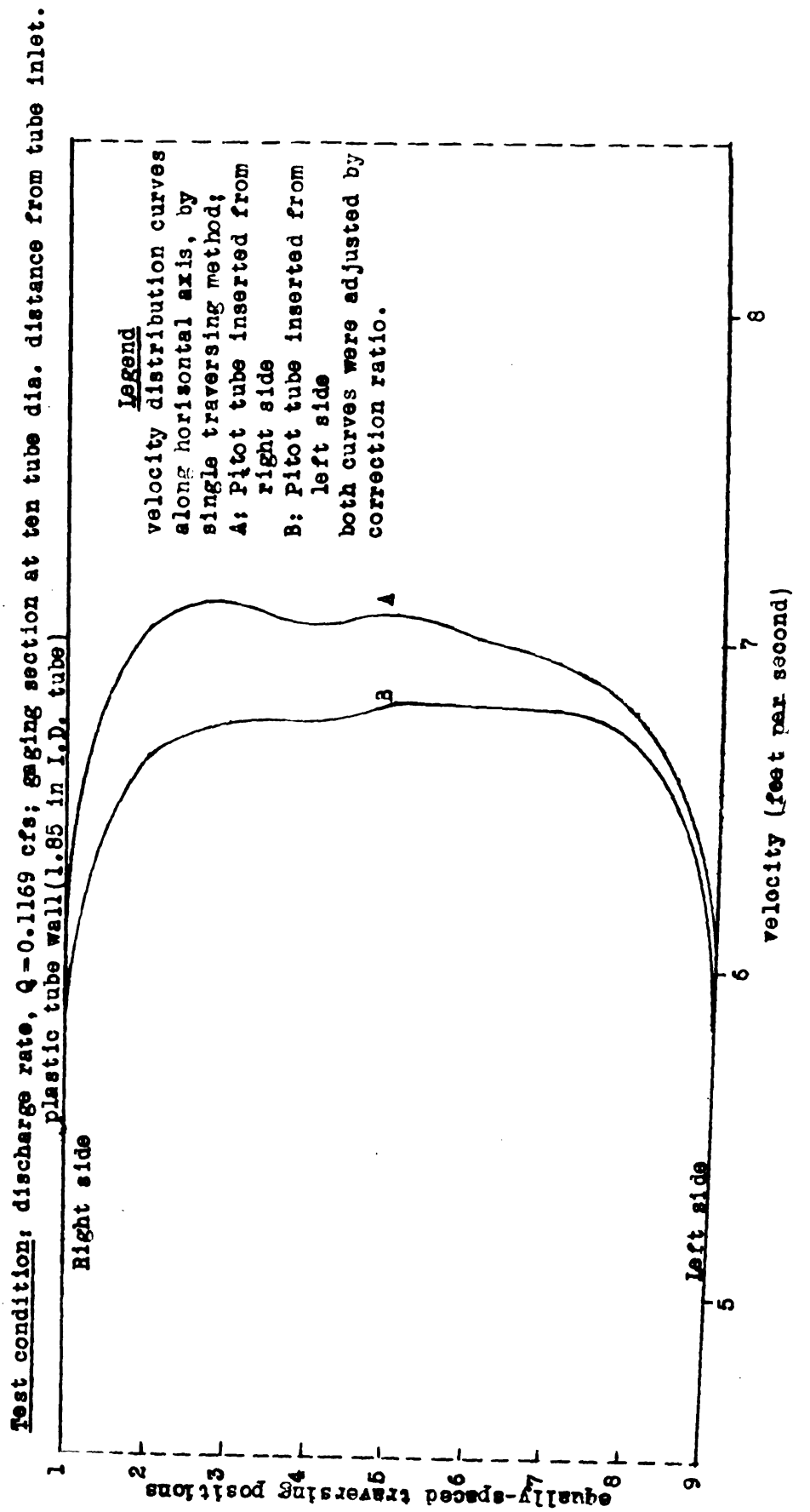

Fig. 23. Velocity distribution curves to show the imperfection of correction ratio for the single traversing method.

method was advantageous in eliminating the variation of the effective cross sectional area and resultant variation in velocity due to the stem effect. However, it possessed the disadvantage of causing a measured velocity due to the existance of the turbulent wake at the static pressure opening in the trailing tube.

D. Calibration of the Pitot-static Tubes

In this study, the procedure was to measure the mean velocity with the double traversing method and to compare it with the true mean velocity as determined by weighing tank measurements. Flow system No. 2 with constant head was used. The mean velocity ranged from 6.260 to 8.057 fps. During the traverse, continuous weighing-tank measurements were made to determine the true mean velocity, and to investigate the discharge variation. It was noted that the discharge variation was about 0.5 - 1.0 per cent, i.e. the variation of velocity. This error was considered as negligible.

For the calibration of the Pitot-static tubes, three sections at 10, 15, and 19 diameters from the entry nozzle of the plastic tube were selected to measure the velocity distribution in the section from two or four directions.

After drawing the corrected velocity distribution curve, the average of the velocities obtained at the center of the area of six rings of equal areas for the two inch plastic tube was taken as mean velocity of the Pitot-static tube. The ratio of the mean velocity thus obtained to the mean velocity determined by the weighing tank is the coefficient. As was expected the coefficient of each Pitot-static tube was different and varied with the change of mean velocity almost inverse-proportionally. The calibration curves are shown in Fig. 24. These four curves were compared with the curves presented by Cola and Pardoe [5] in Fig. 20. The results of this study demonstrated that the slope of the calibration curves were quite

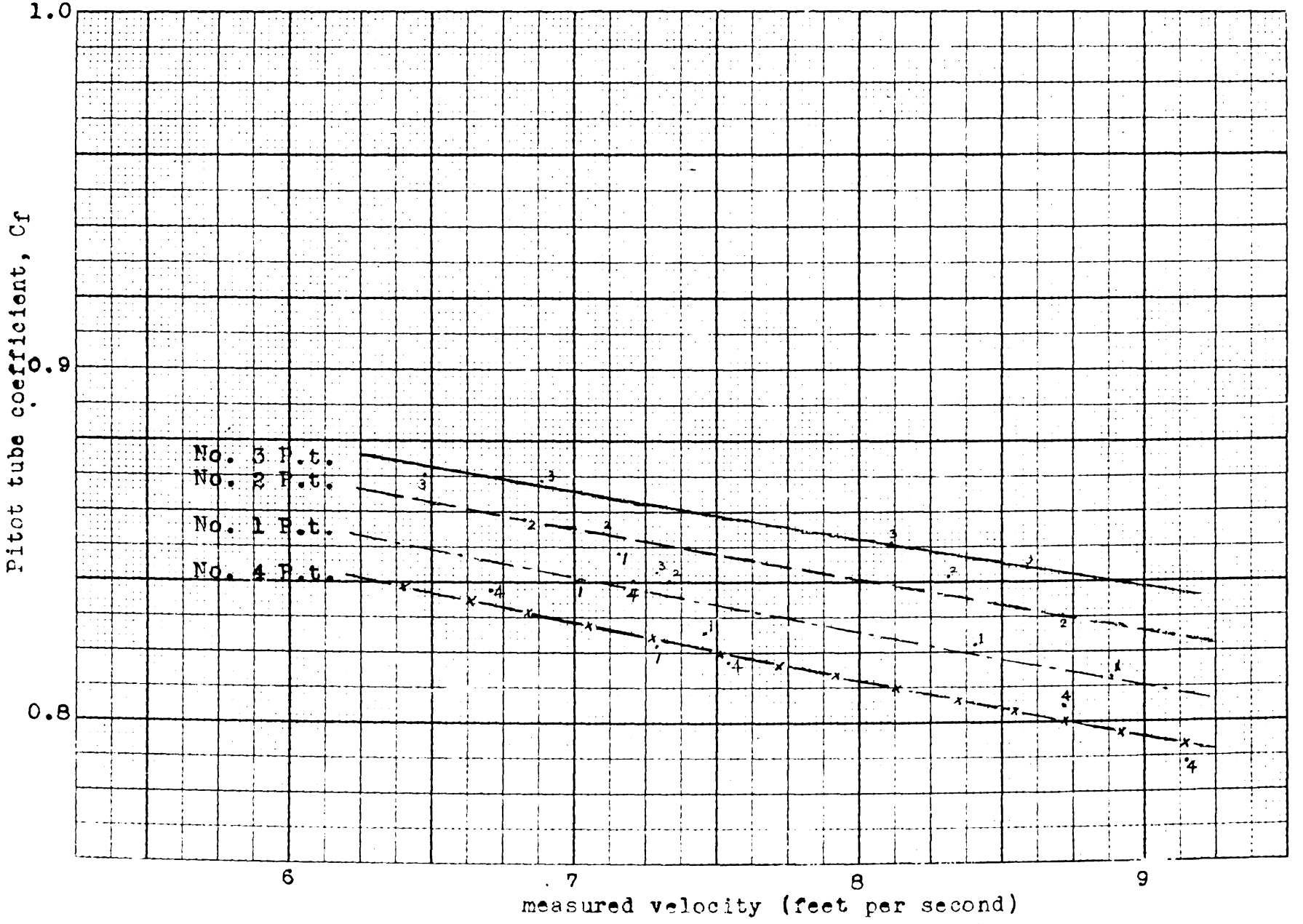

Fig. 24. Results of calibration test of the four constructed Pitot tube in this study.

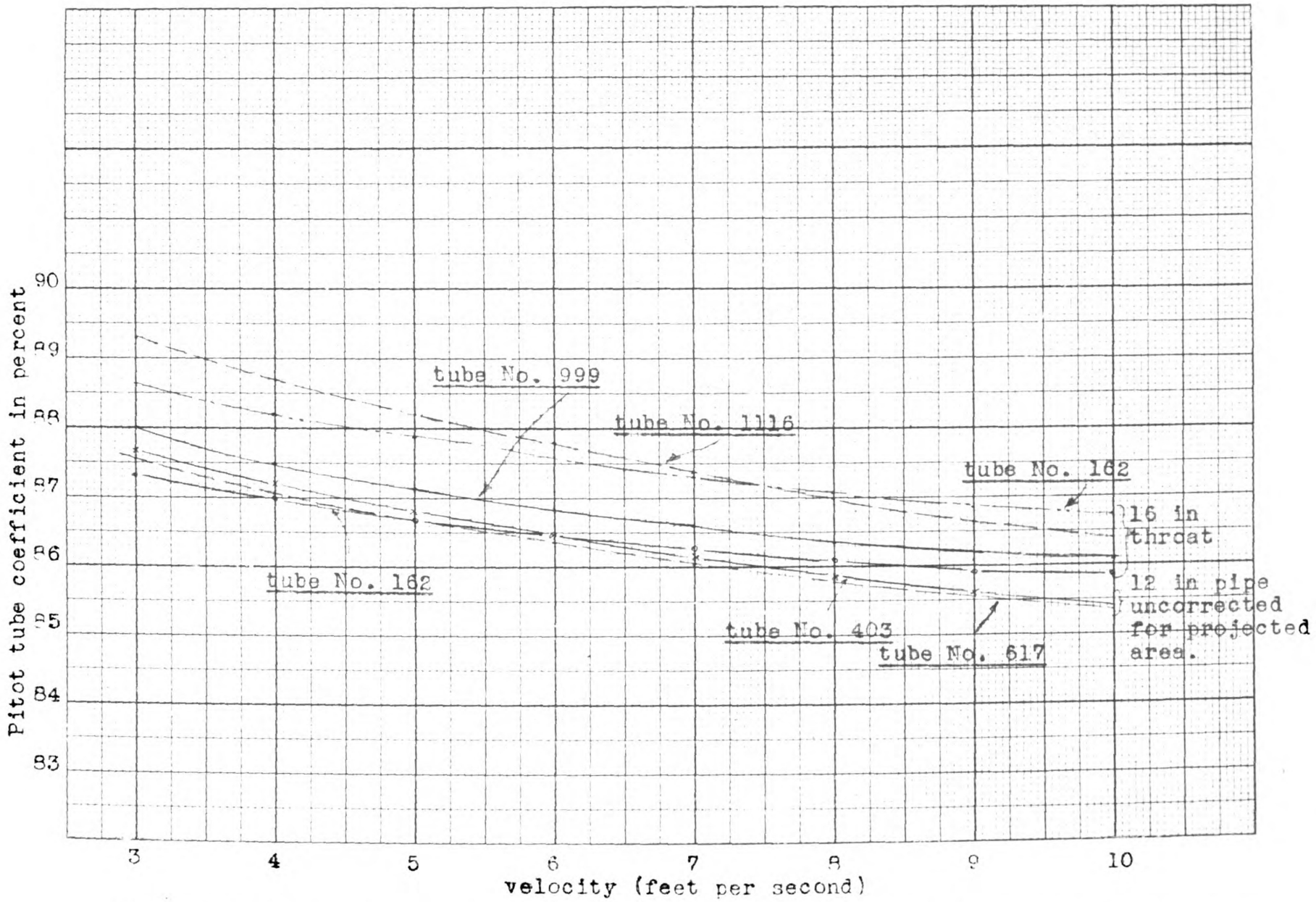

Fig. 20. Results of calibration test of Pitot tubes at Alden Hydraulic Laboratory by Cole(5) in 1930-1934.

similar with that of curves drawn by Cole and Pardoe.

The true velocity will be computed without traversing stem effect from the obtained calibration curves. Four of the measured velocity distribution curves at the section ten diameters distance from the entry nozzle, at the mean velocity of 5.852 fps, were shown in Fig. 25. The distribution curves did not possess symmetry with respect to the center of the plastic tube due to the variation of plastic tube diameter and the bend of the tube. The variation or plastic tube diameter (O.D.) measured at approximately 1.53 per cent and the slight bending of the plastic tube due to gravitational force on the water in the tube both might affect the nonsymmetry of the velocity distribution curve.

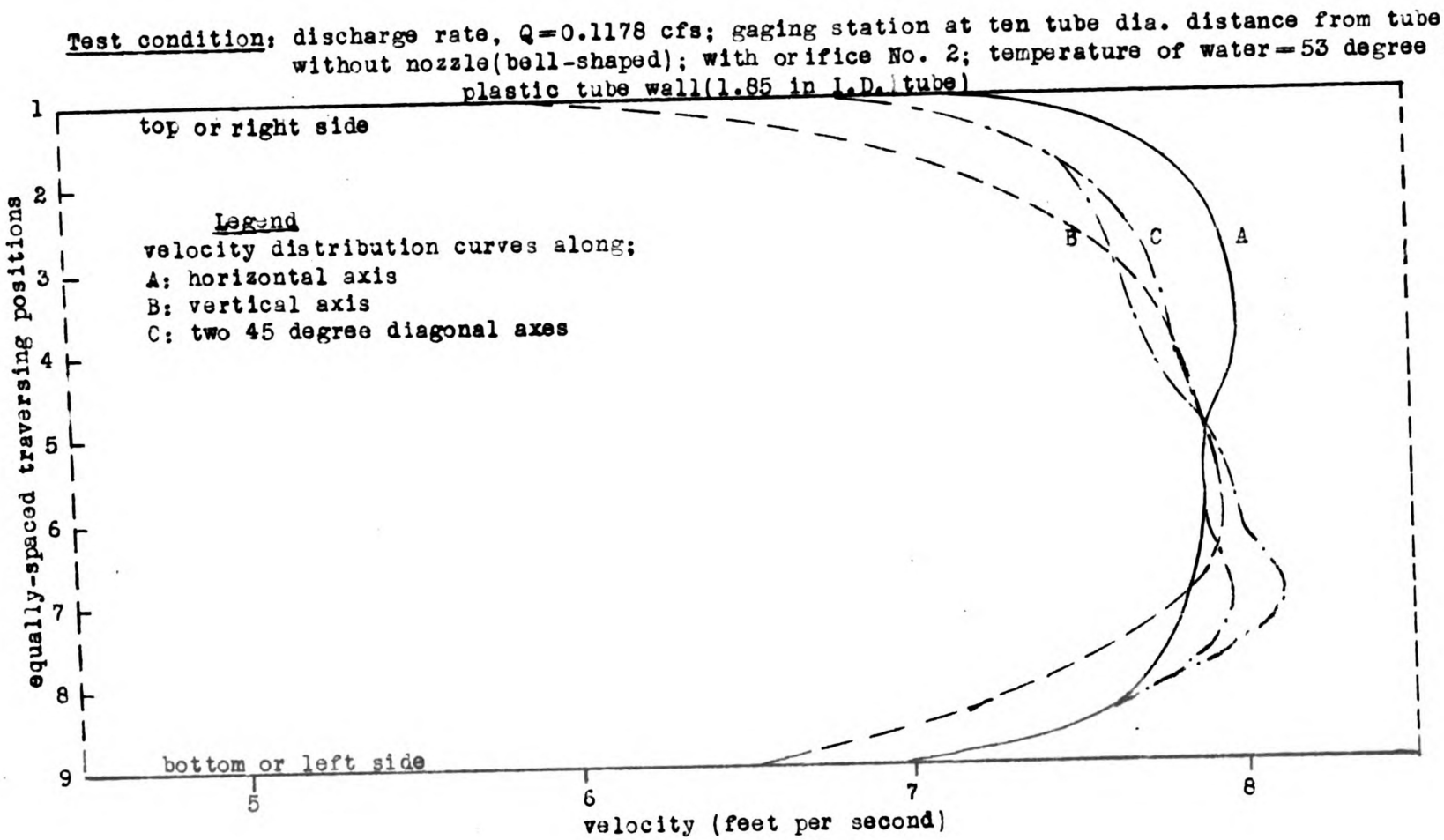

Fig. 25. A example of velocity distribution curves in a gaging section

IV. DISCUSSION OF TURBULENT FLOW IN ENTRANCE REGION OF A CLOSED CONDUIT

As the fluid enters the conduit through a well-rounded entrance or square-edged entrance from a large reservoir, a uniform velocity distribution occurs at the start of the conduit. Through the action of wall friction, a boundary layer is created at the wall, which gradually encroaches on the uniform stream as the flow proceeds down the conduit. As the total flux remains constant, the flow in the undisturbed central core must accelerate to compensate for this retardation of the flow near the wall. This change of stream velocity causes a greater reduction of the static pressure than for the corresponding fully developed flow. The wall friction is also greater than that for the fully developed conduit flow, giving a large gradient of the energy head. The above description of the turbulent flow in the entrance region of a closed conduit was mentioned by Ross [14]. Fig. 26 illustrates the development of the boundary layer and serves to define several of the pertinent quantities.

The fully developed turbulent flow is recognized at the segment behind the boundary layer segment which is occupied by the nondissipative core. When the conduit is of sufficient length to assure the full development of the layer, the thickness of turbulent layer equals the radius of the conduit. In

the study of Pitot tube calibration or measurement of velocity distribution across the section, it was desired to locate the gaging section in the fully developed turbulent flow segment of the conduit, in order to avoid particular turbulent flow at intermediate layer between the turbulent layer and non-dissipative core, in the boundary layer segment. Keulegan [13] demonstrated the relationship between the length of development of boundary layer in rough pipes and the roughness factor, as shown in Fig. 27, where L_b was the length of development of boundary layer in rough pipe, K was the roughness factor, and R was the radius of pipe. According to his figure, if assumed K for plastic tube is 0.00005 referring to Rouse [3] P.405 R is about one inch, then R/K = 20,000. The L_b will be more the 50R or 25 diameters. Therefore the gaging sections at 10, 15, and 19 diameters from the entry were supposed to be within the boundary layer segment, so it was considered that the velocity distribution curves represented ten partially developed turbulent flow profiles.

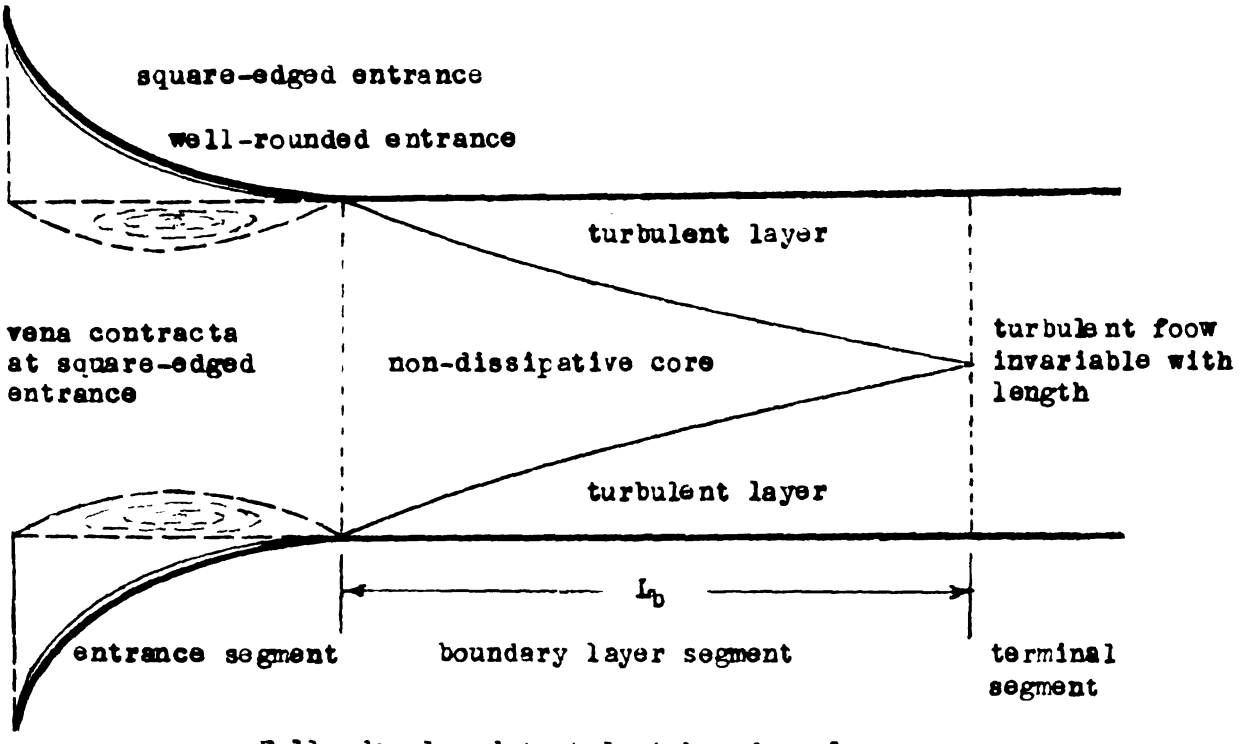

Fig. 26. Schematic diagram of the development of the boundary layer in the entrance region of a closed conduit.

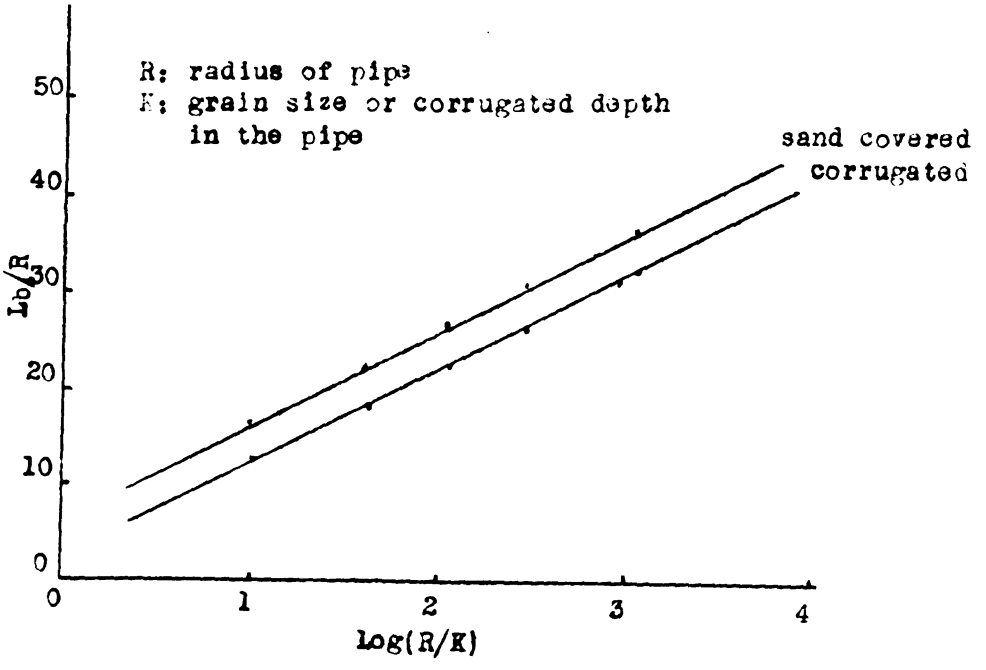

Fig. 27. The relationship between the length of fully developed boundary layer in rough pipes and the roughness factor. (by Keulegan 13)

VISUALIZATION OF SECONDARY FLOWS IN BEND OF A CLOSED CONDUIT

I. Introduction:

It was recognized from previous study that when fluid flows through a bend or curved conduit, the flow pattern becomes more complex than in a straight conduit and is characterized by an altered velocity distribution and the development of longitudinal vortices or secondary flows.

As a primary study of secondary flows, it was aimed to observe the phenomena of secondary flow in the bend. Several visualization techniques were quite effectively employed to indicate the streamline of secondary flows along the boundary layer close to the wall of the bend and some phenomena in the interior of the bend.

II. Methods and Results:

Flow system No. 1 and 2 with 30 degree bent plastic tube, five feet long, was provided for this test.

1) Dye method: For the observation of laminar and turbulent flow, dye method is frequently applied. The attempt to show up the streamlines of secondary flows by injecting dye into the flow of flow system No. 1 did not succeed with a satisfaction. The potassium permanganate solution was injected into the flow by syringe through a fine hypodermic needle at the entrance section of the bend. The injection was made

at several positions across the section.

Because of the turbulent condition in the flow, the dye was rapidly dispersed into the whole section after passing the center of the bend, so that it was difficult to distinctly observe the flows at the bend. However there was a slight difference when the dye was injected at the center of the tube as opposed to the dye injected at the boundary layer close to the wall of the tube, but it was impossible to identify and describe, because of its unstable condition. It was noted that the interior flow curved toward the bottom wall near the end of the bend at a radius larger than that of the tube. After passing the bend, the diffusion of dye began at the portion near the bottom wall of the tube, then the whole tube was full of diffused dye, and identification was no longer possible.

2) Sand method: Fine sand was supplied as suspended material in the flow. This method failed in the visualization of the secondary flow due to the difficulty of obtaining a continuous and linear supply of sand by injection. The instantaneous passage of sand through the bend was difficult to observe by eye or regular camera.

3) Air bubble method: Air bubble injection was applied under lower static pressure of three to five inches of water column in flow system No. 2. This method was more effective than the sand method in showing the flows. Because of the low static pressure on the tube. It was easier to control the continuous bubble supply with a small amount of compression on the injector. The air bubbles were regulated into a small

size of approximate 0.03 inch diameter, so as to eliminate the effect of buoyancy. The route of the air bubbles passing the bend was sketched schematically in the vertical and horizontal planes in Fig. 28. The air bubbles generally followed the interior flow rather than the boundary layer flow close to the tube wall. The trend of the interior flow in the vertical plane in the bend is described as follows: after the flow got to the bend, the interior streamlines rapidly approached the tube curvature, although the boundary streamlines followed a spiral path. Near the end of the bend, the interior streamlines curved inward toward the bottom wall of the plastic tube at a radius larger than the diameter of the tube, and continued to curve perceptively for about one tube diameter or more distance downstream from the end of the bend. Thereafter, the streamlines returned close to the center line of the tube with a curvature at a radius smaller than the diameter of the tube, toward the top wall of the tube. In the horizontal plane at the end of the bend, these air bubbles were carried toward the center line of the tube.

From the observation, it was indicated that the flow, at least in the region away from the top and bottom walls, tended to follow a combination of two dimentional potential flow patterns.

4) Colored thread method: This test was conducted with flow system No. 1. The suspension of colored threads one and two feet long in the flow was attempted. At portions of the

bend and a short distance downstream from the bend, the threads showed essentially the same streamlines of interior flow that were observed by the air bubble method. But the threads did not follow the route of the air bubble passage at the points some distance beyond the bend. The threads laid along the bottom wall of the tube after it formed the curvature pattern from the top to the bottom wall at the end portion of the bend. The threads that were attached to the side close to the top inside wall or bottom inside wall, tended to approach the bottom wall and to lie along the wall. The utility of the thread method of visually observing the flow pattern is limited because of:

(a) the restraint on the thread since it is attached to the wall,

(b) the viscosity effect of the flow attempting to move the thread with it,

(c) the thread in effect shows a resultant position rather than the true streamlines.

5) Paint method: Flow system No. 1 was applied for this test. Satisfactory pictures of the pattern of secondary flows in the boundary layer close to the tube wall were taken. A coat of white paint approximately 0.01 inch thickness was placed on the inside wall of the plastic tube. Water flow was then immediately imposed on the paint. The pattern of secondary flow in the boundary close to the inside wall of the tube was impressed on the fresh paint.

The streamline curvature commenced between one half and

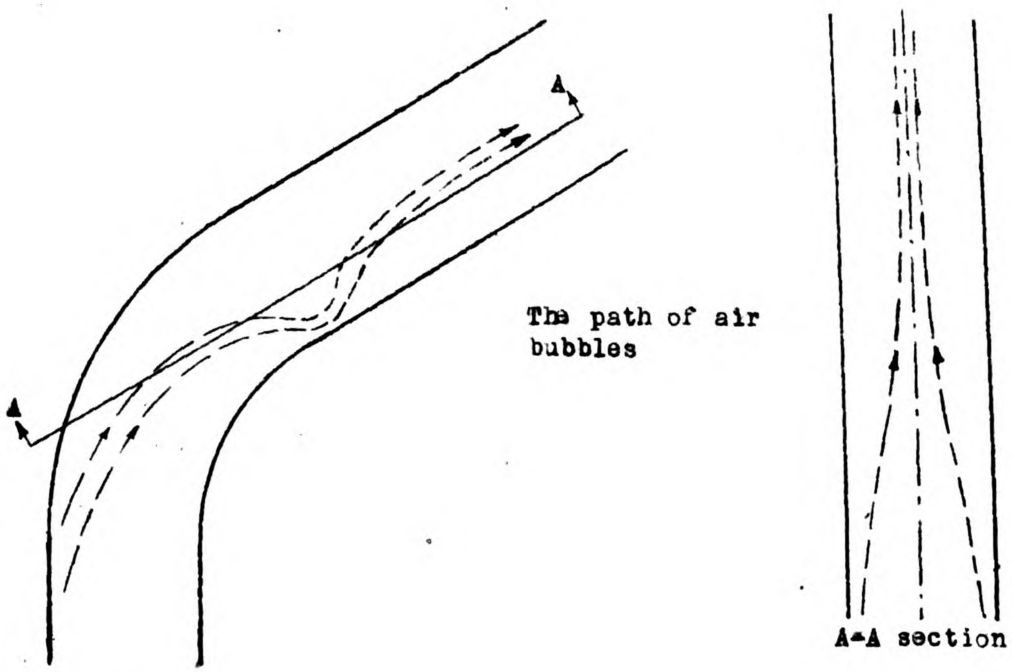

Fig. 28. Schematic diagram of interio. flow at the bend in vertical and horizontal planes.

Fig. 29. Side view of secondary flows in the boundary near the tube wall at the bend.

one tube diameter upstream from the bend. The boundary streamlines in the proximity of the bend as shown by this paint method showed gradually more curvature of flow than those in the interior as was observed by the air bubble method. The flow in the boundary near the wall was diverging to the right and left with respect to the top wall of the tube. Thereafter two distinct spirals were shown on the tube wall at the bend symmetrically, as shown in Fig. 29 and 30.

In Fig. 31, the bottom wall showed that the boundary streamlines at the bend symmetrically converged from both sides toward the center line of the bottom wall.

The disadvantage of this method was that the paint was quite difficult to remove after the test.

6) Oil-sand method: A second method making possible the visualization of secondary flows was by mixing thick oil with sand and coating the interior tube wall. The oil and sand was much easier to wash out with cleaners and gave essentially the same patterns of secondary flows which was noted with the paint method. This test was conducted with flow system No. 2.

7) Plastic powder method: Green plastic powder which has the specific weight of about one gram per cubic centimeter, was mixed with the water in flow system No. 2. This insoluble plastic powder moved through the system as granular-type clusters. These clusters followed the same pathway as the air bubbles, when they moved through the bend section. The test provided a confirmation of the reliability of the small air bubble method.

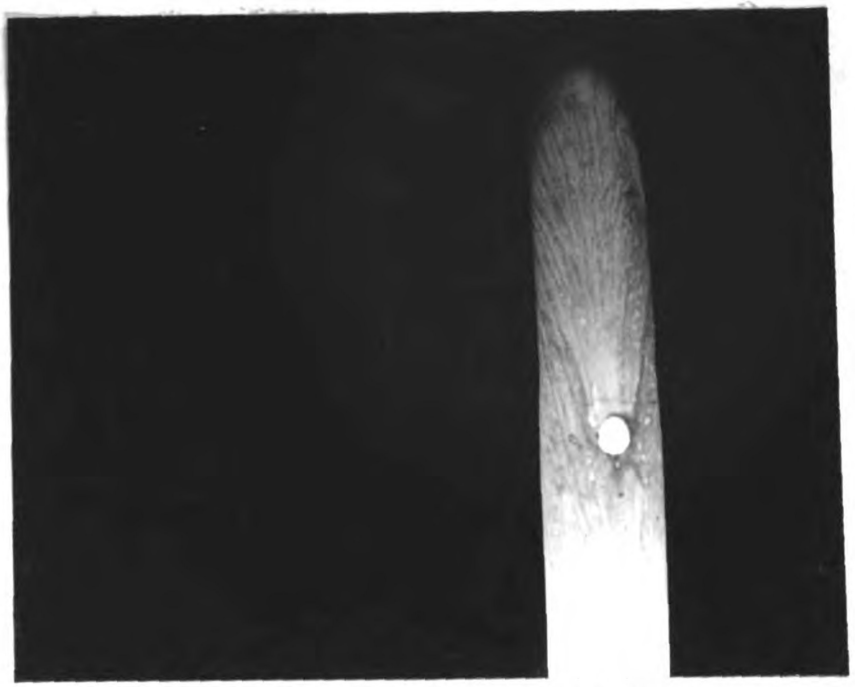

Fig. 30 Top view of secondary flows in the boundary near the tube wall at the bend.

Fig. 31 Bottom view of secondary flow in the boundary near the tube wall at the bend.

III. Discussion

The phenomena of secondary flows in the boundary close to the tube wall and in the interior of the bend and in the extension tube beyond the bend were effectively visualized by the paint method, oil-sand method, air bubble method, and green plastic powder method. It was noted that the interior flow and the boundary flow in the bend are distinctly separated with different spirals, due to the difference in viscosity effects at the boundary close to the tube wall and the interior. Down stream from the main double spirals, at the bend there was some separation effect on the layer near the bottom wall due to the return flow in the interior from the main spirals. Further investigation is necessary to study this separation effect.

S

in sp

the r

its c

were

study

sente

I. I

II

SUMMARY

Since it was recognized that one of the important factors in sprinkler distribution is the secondary flows at the bend in the rotary sprinkler, the study of hydraulic instruments and its construction, and the visualization of secondary flows were conducted in this project for the further purpose of the study in secondary flows. The results of this test are presented as follows:

I. Five mm regular soft glass tube was chosen for use in this study as the proper size of manometer tube. The error of time lag on the readings was eliminated by allowing two minutes to elapse thus establishing steble reading in the manometers. The variation of capillary rise in the nominally similar sized manometer tube was adjusted by a calibrated scale shown in Fig. 16. Three types of manometers were constructed: A) the vertical piezometer tubes for tube wall static pressure, B) 30 degree inclined mercury manometers because the velocities ranged from three to eight fps, and C) 30 degree inclined piezometer tubes for the lower velocities from less than one to three fps. The devices for capacity and resistance damping were provided with mercury and one mm capillary tube with screw clamp respectively, in order to damp out the fluctuation of readings in the manometer caused by turbulent flow.

II. 0.030 inch I.D. hypodermic needle was used to construct the

Pitot static tube since the high efficiency in the velocity measurement due to time lag and negligible viscosity effect on water flow in the Pitot-static tube. As shown in Fig. 18, the constructed Pitot-static tubes were designed with a similarity to Cole Pitometer which consists of two tubes made together: one, so-called Pitot tube, for total pressure facing upstream, and the other, so-called static tube, for static pressure facing downstream. However, they are set along a streamline. In structure, the only differences between the Cole pitometer and the author's Pitot-static tube are the following:
A) With the Cole Pitometer, static pressure is measured at the orifice on the tip of the static tube. B) With the author's Pitot-static tube, static pressure was measured at the static openings on the wall of the static tube. In the study of correction for projected area of Pitot-static tube stem that traverses into the plastic tube, the double traversing method was found to be better for correction rather than the single traversing method. In addition the checking process supported the above statement. By the double traversing method with the correction factor for the reduction of cross section of plastic tube, velocity distribution curves at the gaging sections were drawn for the coefficient calibration of Pitot-static tubes as shown in Fig. 24. It was noted that the four similarly designed Pitot-static tubes had different calibration curves, however the slope of the

curves were practically the same.

III. An effective method to visualize the secondary flows in the bend was found. The secondary flow in the boundary close to the wall of the tube was clearly shown on the inside wall of the plastic transparent tube coated with (A) fresh white paint and(B) black oil mixed with sand. The streamlines of the interior flow in the bend was observed by the small air bubble, thread, dye, plastic powder and sand methods. The most effective method to show interior flow was the small air bubble method. The schematic diagram of interior flow is shown in Fig. 28.

BIBLIOGRAPHY

1. Echman, D. P., Industrial Instrumentation, John Wiley & Sons, Inc., New York, 1953, p. 13-14, p. 218-223, p. 105-125, p. 286-290.
2. Addison, H., Hydraulic Measurements, John Wiley & Sons Inc., New York, 1941, p. 14-29, p. 49-63, p. 72-81, p. 156-163, p. 176-181.
3. Rouse, H., Engineering Hydraulics, John Wiley & Sons Inc., New York, 1950, p. 186-202, 209.
4. Vennard, J. K., Elementary Fluid Mechanics, John Wiley & Sons Inc., New York, 1955, p. 15-17, p. 282-293, p. 299, p. 309-310.
5. Cole, E. S., Pitot Tube Practice, ASME Transactions, Vol. 57, 1935, p. 281-294.
6. Folsom, R. G., Review of the Pitot Tube, The University of Michigan Mechanical Engineering Department Report, 1955.
7. Hurd, C. W., Chesky, K. P., Shapiro, A. H., Influence of Viscous Effects on Impact Tubes, Massachusetts Institute of Technology Report, 1951.
8. Ellison Draft Gage Co., A Treatise on the Ellison Pitot Tube and How to Use It.
9. Goldstein, S., Modern Developments in Fluid Dynamics, Oxford Clarendon Press, p. 243-264, p. 312-319, p. 265-285, p. 34-35.

10. Bilanski, W. K., Factors That Affect Distribution of Water from a Medium Pressure Rotatary Irrigation Sprinkler, PhD Thesis in Agricultural Engineering of Michigan State University, 1956.

11. Merrian, K. G., & Spaulding, E. R., Comparative Tests of Pitot Static Tubes, Department of Mechanical Engineering, Worchester Polytechnic Institute, Tech. Note No. 546, of NACA, 1935.

12. Grossman, L. M., & Li Huon, Turbulence Investigation in Liquid Shear Flow By the Method of Electro-Magnetic Induction, University of California, Series 65 Issue 2.

13. Kenlegan, G. H., Theory of Flow Through Short Tubes with Smooth and Corrugated Surfaces and with Square Edged Entrances, Highway Research Board, Research Report 6-B, 1943.

14. Ross, D., Turbulent Flow in the Entrance Region of a Pipe, ASME Paper No. 54-A-39, 1955.

15. Anderson, A. G., Hydraulics of Conduit Bends, St. Anthony Falls Hydraulic Laboratory, University of Minnesota, (Bulletin No. 1), 1943.

16. Silberman, E., The Nature of Flow in an Elbow, St. Anthony Falls Hydraulic Laboratory, University of Minnesota, Project Report No. 5, December, 1947.

Note:

[ ] was used to identify the number in the above list in this thesis.